Characterization of L-glutamate uptake in the freshwater sponge *Ephydatia muelleri*

by

Zachary James Dumar

A thesis submitted in partial fulfillment of the requirements for the degree of Master of Science

in

Systematics and Evolution

Department of Biological Sciences

University of Alberta

Abstract:

Animals use a variety of different means to integrate environmental cues and to coordinate responses to these cues. In sponges (phylum Porifera) this capacity for response is limited by the absence of nervous or endocrine systems. Despite this, sponges are capable of whole-body responses that require coordination of the action of multiple tissues and organs. The freshwater sponge *Ephydatia muelleri* undergoes an expansion-contraction "sneeze" response upon application of irritants or mechanical stimulation that flushes water out of its aquiferous system. Previous work has found that the amino acid L-glutamate specifically triggers this response at concentrations above 70 μM, and that incubation with GABA prevents the sneeze response from occurring. However, little is known regarding how L-glutamate passes into the body of *E. muelleri*. This thesis focused on characterizing the rate and functional characteristics of L-glutamate uptake by *E. muelleri* through use of radioisotope uptake. Uptake of L-glutamate by *E. muelleri* is specific at low L-glutamate concentrations with two putative transporters acting (K_m = 8.77 μM, J_{max} = 64.24 pmol L-Glu mg protein^{-1} min^{-1}; K_m = 2.87 μM, J_{max} = 25.1 pmol L-Glu mg protein^{-1} min^{-1}). L-glutamate uptake is reduced in the presence of D-glutamate and L-aspartate, but shows low or no dependence on sodium, calcium, or protons. Bioinformatic analysis identified two putative SLC1-like transporters and eight putative transporters resembling SLC17 transporters in the *E. muelleri* genome. These results support a case of uptake of an amino acid in a freshwater environment. The localization of uptake in the body of *E. muelleri* is currently unclear, but the rate of uptake suggests that the observed L-glutamate uptake does not directly contribute to triggering the sneeze response in *E. muelleri*.

Preface:

The contents of this thesis are arranged in the manner of a single publication, without a dedicated introduction or discussion chapter. The intent is for the data contained in this thesis to be formatted into a publication to be submitted to a scientific journal with the thesis author (Zach Dumar) as the primary author and the secondary authors being Drs. Greg Goss, Tamzin Blewett, and Sally Leys.

So long, and thanks for all the fish.

Douglas Adams, *The Hitchhiker's Guide to the Galaxy*

Acknowledgements:

First and foremost, I would like to thank Dr. Sally Leys for her support for these last two and a half years in experimental design, provision of supplies, and commentary on various writings. I also thank Dr Greg Goss for the use of his lab facilities for the majority of the work contained in this thesis, and Dr. Joel Dacks for access to his data cluster for bioinformatics analyses and his commentary that shaped the phylogenetic tree contained in this thesis. For their input during lab meetings and their support over the last several years, I would like to thank the following past and current members of the Leys lab: Dr. Amanda Khan, Jasmine Mah MSc, Lauren Law MSc, Lauren Grombacher, Nathan Grant MSc, Curtis Dinn MSc, Raz Moskovitch, Azraj Dahihande, Dr. Vivian Vasconcellos, Amy Zhang, Nikita Sergeenko, Pablo Aragones-Suarez, Kira More, and Ciara Verstraete. I thank Drs. Tamzin Blewett and Chris Glover for their help in training me in radioisotope work and their commentary on experimental approaches. I would also like to thank the other members of the Goss lab for their assistance navigating their lab space and their support in my endeavors. Finally, I would like to thank my friends from the University of Alberta Pokémon Club and Quiz Bowl Team for putting up with me for the last two and a half years, and my family (especially my father) who were there to emotionally support me and provide needed provisions and numerous trips to and from the airport.

Table of contents:

List of tables:

List of figures:

Glossary of Terms:

Active transport: movement of a substrate against a concentration gradient, involving the use of either consumption of energy or movement of a different substrate down its concentration gradient.

Diffusion: Movement of a substrate down a concentration gradient.

Transport: Net movement of a substrate across a cell membrane. This reflects either facilitated diffusion through a pore or channel or active transport.

Uptake: Net movement of a substrate from the environment into an organism. This can reflect diffusion or active transport.

1. Introduction:

1.1 Body coordination of non-bilaterians:

All animals require a means to coordinate a response to changes in their environment. The basis for this capacity must have been present in the common ancestor of all animals and understanding the components that may have contributed to these mechanisms is important for understanding early evolution of animals. Insights into how early animals may have responded to their environment can be gained from studying the extant non-bilaterian phyla: Cnidaria, Ctenophora, Placozoa, and Porifera. The determination of which of these four phyla is sister to remaining Metazoa is a continued topic of contention. Sponges (phylum Porifera) were originally thought to be the sister to other metazoans based on morphological complexity (Nielsen 2008), but as the genomic era has progressed evidence has accumulated for the possibility of ctenophores (and to a lesser extent placozoans) as being the sister group (Dellaporta et al. 2006, Whelan et al. 2015, Simion et al. 2017, Figure 1). The resulting position of the phyla in analyses depends greatly on factors such as sampling of different groups and filtering of reads, and advances in sequencing technology and greater diversity in organisms to draw sample data from will help to further clarify this question in the future. However, even without knowing which phylum is sister to the other metazoans, insights can still be gained from examining the coordination systems of these extant animals.

Two of the four non-bilaterian phyla, ctenophores and cnidarians, have nervous systems. In cnidarians these nerves are organized as a nerve net that branches throughout the body of the organism. This nerve net can be used to coordinate a variety of different behaviors, including feeding and locomotion (Satterlie 2015). The major signaling

molecules used in cnidarian nervous systems include nitric oxide, catecholamines, and a variety of neuropeptide hormones (Dewaele et al. 1987, Gajewski et al. 1998, Anctil et al. 2005). Ctenophores similarly make use of nerve nets in coordinating their body responses (Jager et al. 2011). However, the underlying signaling molecules used in the nervous system of ctenophores differ from cnidarians. This includes a dramatic expansion in ionotropic glutamate receptors (iGluRs), and no capacity for catecholamine based signaling (Moroz et al. 2014). This expansion along with other lines of evidence such as the absence of bilaterian developmental signaling genes has led to the hypothesis that ctenophore nervous system evolution may have occurred independently of other animals, and that eumetazoan nervous systems had an independent origin from the ctenophore nervous system (Moroz 2015). Placozoans in contrast to cnidarians and ctenophores lack a nervous system but are still capable of utilizing peptide based signaling molecules to coordinate their feeding response and body movement (Senatore et al. 2017).

Sponges, like placozoans, lack a nervous system. The body of a sponge consists primarily of two tissue types: the pinacoderm and the choanoderm. The choanoderm consist of a series of canals with flagellated choanocyte chambers that drive water flow from incurrent ostia on the outside of the sponge to excurrent oscula (Leys and Hill 2012). The pinacoderm can be split into three different tissue types: The basopinacoderm which forms the site of attachment of the sponge to the substrate, the exopinacoderm that forms the outer epithelium of the sponge, and the endopinacoderm which lines the choanoderm (Leys and Hill 2012). The endo- and exopinacoderm are bridged by a space known as the mesohyl, where a variety of motile cells carry out processes such as spicule production and collagen excretion (Simpson 1984) Most sponges are obligate filter

feeders, extracting bacteria from the water that flows through their bodies (Reiswig 1975). The one exception to this is carnivorous sponges, which utilize their spicules to capture prey and then subsequently digest it (Vacelet and Boury-Esnault 1995). One class of sponges, Hexactinellida (glass sponges), is capable of electrical signaling and propagation of action potentials through syncytial tissues (Mackie et al. 1983, Leys et al. 2007). This signaling in glass sponges can be used to start and stop the pump system in response to sediment clogging the filtration mechanisms (Leys et al. 1999, Grant et al. 2019).

Cellular sponges are also capable of whole body coordinated responses. The demosponge *Tethya wilhelma* undergoes rhythmic body contractions that affect the whole sponge (Nickel 2004). The period of these contractions can be modulated by compounds that are neuroactive in other organisms including caffeine and nitrous oxide (Ellwanger and Nickel 2006, Ellwanger et al. 2007). Recently, work in another demosponge *Halichondria panicea* has found that the sponge's contractile response is modulated by the amino acid L-glutamate and GABA (Goldstein et al 2020).

Another experimental system for the study of reactivity of sponges is the freshwater sponge *Ephydatia muelleri*. Exposure of *E. muelleri* to either mechanical stimulation or an irritant such as ink causes the entire sponge to undergo an expansion-contraction "sneeze" response that forces water out of the entire aquiferous system (Elliott and Leys 2007, Figure 2). The osculum of the sponge serves an important role in the sneeze response, as the first portion of the sponge to react upon stimulus is the osculum and removal of the osculum prevents the response (Ludeman et al. 2014). Further work found that the amino acid L-glutamate specifically triggers the sneeze

response at concentrations above 70 μM, and that incubation of the sponge in GABA prevents the sneeze response from occurring (Elliott and Leys 2010). This suggests that a L-glutamate based signaling system is involved in coordinating the sneeze response, as the functional coupling of GABA synthesis from glutamate is an important backbone of glutamate based signaling systems (Hertz 2013).

The high concentration of L-glutamate required to trigger the sneeze response heavily contrasts with the concentration of L-glutamate found in ambient water. L-glutamate concentration in freshwater is typically on the scale of 5 nM to 1 μM, which is far below the minimum threshold concentration of 70 μM to trigger the sneeze response (Abe and Wasa 1989, Robarts et al. 1990, Hornak et al. 2016). Decomposition of an organism near a sponge could locally increase the dissolved amino acid concentration, but this increase cannot be readily quantified (Thomas 1997). The intracellular L-glutamate of *E. muelleri* has not been examined, but previous work in marine sponges has identified an effective concentration range of 205 nanomoles to 14 micromoles of L-glutamate per gram dry weight of tissue (Sica and Zollo 1977). The threshold concentration of 70 μM L-glutamate to trigger the sneeze response is also much lower than the mM concentrations of L-glutamate utilized in the synaptic cleft of vertebrates and in the glutamate signaling systems of plants (Dzubay and Jahr 1999, Moussawi et al. 2011, Qiu et al. 2020).

Transcriptomic analysis of a variety of sponge species has previously found the presence of metabotropic glutamate receptors(mGluRs) within sponges, providing the backbone for a glutamate based signaling system within sponges (Riesgo et al 2014). The ability of AP3 and kynurenic acid, inhibitors of glutamate receptors, to attenuate or

prevent entirely the sneeze response by *E. muelleri* provides further evidence for a coordinated L-glutamate signaling system to be the basis of the response (Elliott and Leys 2010). However, little is currently known about how L-glutamate is entering into the body of the sponge during these experiments (Figure 3).

E. muelleri has a functional epithelial barrier for solutes, so diffusion alone would not be expected to be sufficient to provide L-glutamate for a signaling system (Adams et al. 2010). The focus of this thesis was to determine whether L-glutamate was taken up from the ambient water by *E. muelleri*, and if so then whether uptake was specific and at what rate uptake occurs. The requirement of ions as a driving gradient for uptake was then evaluated.

1.2 Amino acid transport in animals:

A variety of different aquatic animals have been documented to take up amino acids across their extra-intestinal epithelia (reviewed in Wright and Manahan 1989). A frequent site of extra-intestinal uptake is across the gills, as the water flow occurring through the gills allows for access to a large amount of substrate to transport (Wright 1988, Glover et al. 2011, Blewett and Goss 2017). The primary purpose of the taken up amino acids is as food, such as occurs with larval bivalves and sea urchin embryos (Epel 1972, Rice et al. 1980). Amino acid uptake is often dependent on ions in the environment to provide a net driving gradient, as amino acid concentrations intracellularly are much greater than those typically found in the environment (Robarts et al. 1990, Thomas 1997, Kuznetsova et al. 2004). The major ion most often coupled to transport is sodium and reducing sodium in seawater impedes amino acid uptake in organisms ranging from crabs to cnidarians to echinoderms (Epel 1972, Buck and Schlicter 1987, Blewett and Goss 2017). This presents a challenge when amino acid

uptake is occurring in freshwater environments, where sodium concentrations are around 150 μM (Dugan et al. 2017). This low level of sodium is not high enough to act as a driving gradient for amino acid uptake, as intracellular sodium concentrations are in the range of mM (Morgan et al. 1994). However, many freshwater organisms actively take up sodium from the environment, and amino acid uptake could be directly coupled to this sodium uptake (Horne 1967, Dietz 1979, Murua 2007). Another possibility for uptake remains in proton gradients due to different pH levels. The possibility of several different ion gradients contributing to L-glutamate uptake led to the examination of the effect of sodium, calcium, and protons on the uptake capacity for L-glutamate of *E. muelleri*.

Along with functional experiments, studies in vertebrate systems have also identified a suite of proteins involved in amino acid transport. Amino acid transporters are part of a larger group of 65 families of proteins known as solute carriers (SLC) that take up a wide variety of different compounds (Fredriksson et al. 2008, Bai et al. 2017). The majority of SLC transporters are also dependent on an ion gradient across the cell membrane to facilitate uptake (Hoglund et al. 2011). Of the seven families of SLC transporters that transport amino acids, four families of SLC transporters contain members capable of L-glutamate uptake: SLC1, SLC3, SLC7, and SLC17 (Figure 4). SLC1 transporters are excitatory amino acid transporters (EAATs) and are found in neurons to sequester L-glutamate from the synaptic cleft (Kanai et al. 2013). Transport of L-glutamate by SLC1 transporters is coupled with sodium and proton import and potassium export, so all three of these ions are required for proper SLC1 function at human synapses (Zerangue and Kavanaugh 1996). SLC1 transporters do not exclusively

transport L-glutamate, in that they are also able to take up the other negatively charged amino acid L-aspartate (Canul-Tec et al. 2017).

SLC3 and SLC7 families form heteromeric complexes together that act as single amino acid transporters (Fotiadis et al. 2013). Most SLC3/7 complexes transport cationic amino acids, but SLC7A13 does transport both L-aspartate and L-glutamate without the need for an ionic gradient (Matsuo et al. 2002). In humans, expression of SLC7A13 is localized primarily to the proximal and distal convoluted tubules of the kidney, where it is used for reabsorption of amino acids before production of urine (Matsuo et al. 2002). SLC17A6-8 are vesicular glutamate transporters (VGLUT), responsible for sequestration of L-glutamate into vesicles in glutaminergic neurons in both vertebrates and invertebrates (Reimer 2013, Jing et al. 2015). VGLUT transport is dependent on chloride ions and is specific to L-glutamate (Reimer and Edwards 2004). There is also some evidence for the capacity of sialin (SLC17A5) to transport L-glutamate and L-aspartate, so sialin is also another potential transporter of interest (Miyaji et al. 2008).

Analysis of the SLC transporter complement of the *E. muelleri* genome was conducted searching for the above identified transporters to provide additional insight to the functional uptake data collected. Comparison of the amino acid transporter complement in *E. muelleri* with the functional characteristics of L-glutamate transport can then be used to identify the likely candidate transporters acting in the sponge. However, since this data is extrapolated from mammalian systems caution should be taken in the assumption of characteristics of the transporters since sponges have been independently evolving from mammals for an extremely long time (Mah and Leys 2017).

1.3 Thesis objectives and methodological summary:

The objective of this thesis was to identify the rate and functional characteristics of L-glutamate uptake by *E. muelleri*. This first involved confirming specific uptake of L-glutamate was occurring rather than diffusion. Comparison of the rate of uptake of L-glutamate with the uptake rate of the large sugar polymer inulin was done to determine this. Then changes in the rate of uptake were assessed at both varying incubation times and varying L-glutamate concentrations to give a maximum velocity of uptake (J_{max}) and the concentration of L-glutamate at which half the maximal rate of uptake is occurring (K_m). This analysis was done using ^{14}C radiolabeled L-glutamate application to sponges and scintillation counting of samples after washing of the surrounding media to lower residual signal. Further analysis of the functional properties of L-glutamate transporters was then done through competitive inhibition experiments using other amino acids and modification of the ionic contents of the surrounding media to determine effects on the rate of L-glutamate uptake. These analyses were coupled with a bioinformatic analysis of the *E. muelleri* genome for SLC transporter genes to determine possible candidates responsible for observed L-glutamate uptake. These investigations provide insight into the ability of freshwater sponges to take up amino acids in freshwater and provide the basis for a glutamate based signaling system.

A

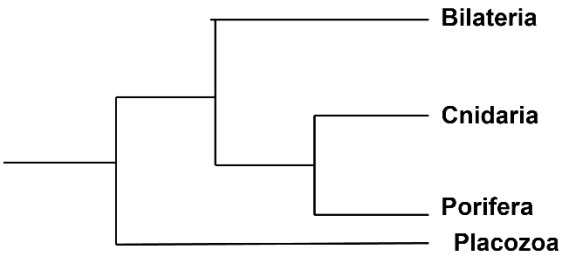
Bilateria
Cnidaria
Porifera
Placozoa

B

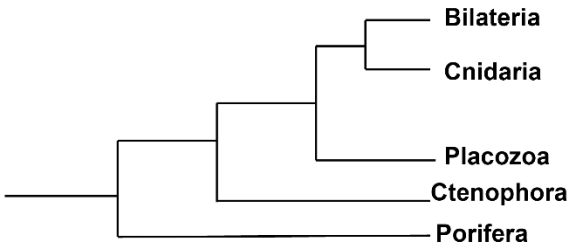
Bilateria
Cnidaria
Placozoa
Ctenophora
Porifera

C

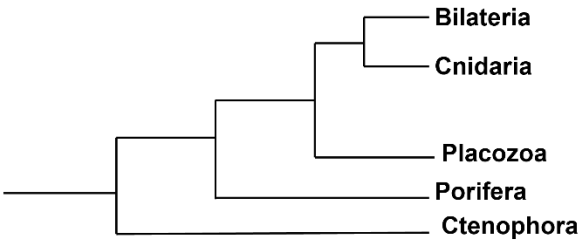
Bilateria
Cnidaria
Placozoa
Porifera
Ctenophora

Figure 1: Illustration of possible topologies of the metazoan tree adapted from Dellaporta et al. 2006 (A), Simion et al. 2017 (B), and Whelan et al. 2015 (C). A: Scenario in which placozoans are sister to all other metazoans and ctenophores included as a monophyletic group with cnidarians. B: Scenario in which sponges are the sister group, with ctenophores diverging before cnidarians. C: Scenario in which ctenophores are the sister group.

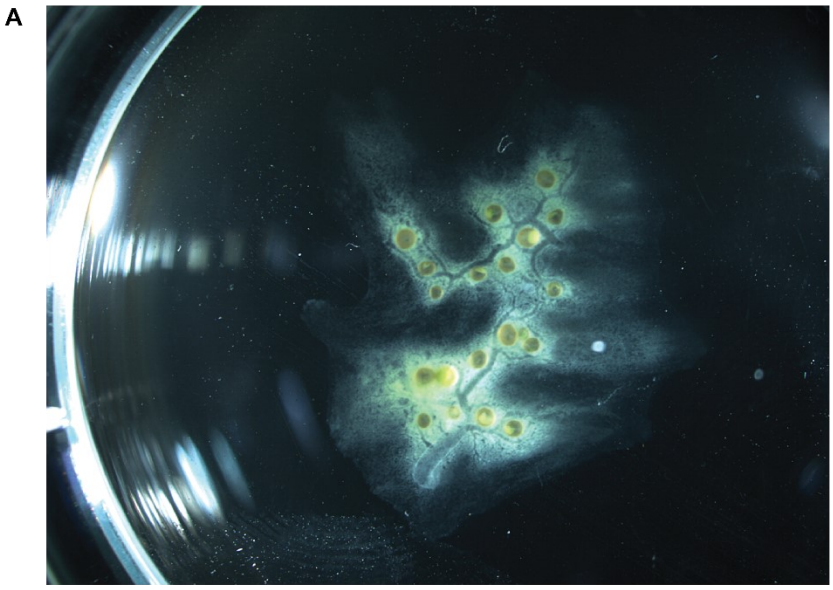
A

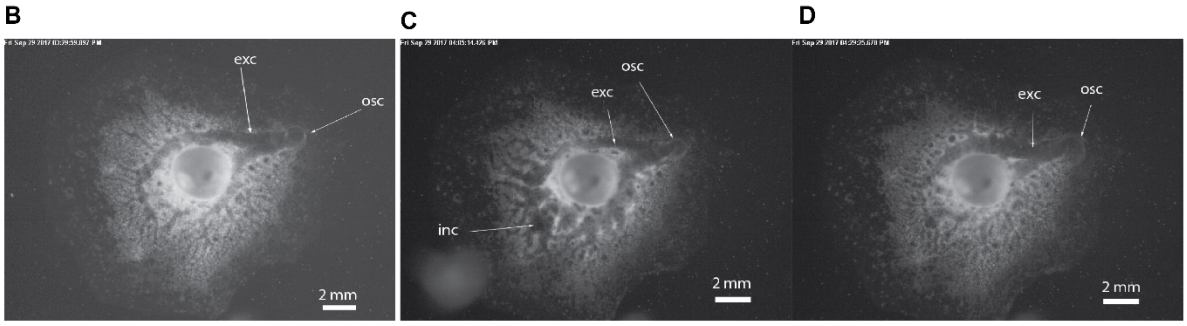
B
exc
osc
2 mm
C
osc
exc
inc
2 mm
D
exc
osc
2 mm

Figure 2: *Ephydatia muelleri* morphology and the sneeze response. A: Representation of a collection of individual sponge gemmules fused into one individual. Similar collections of gemmules were used in the radioisotope experiments. B-D: Time series showing the sneeze response of an individual sponge. B: A sponge prior to the start of the sneeze response. C: Sponge undergoing the expansion portion of the sneeze response D: Sponge near the end of the contraction portion of the sneeze response. 75 μM L-glutamate was added immediately before image B was taken. Scale bar in D represents 2 mm. Excurrent canal (exc), incurrent canal (inc), osculum(osc).

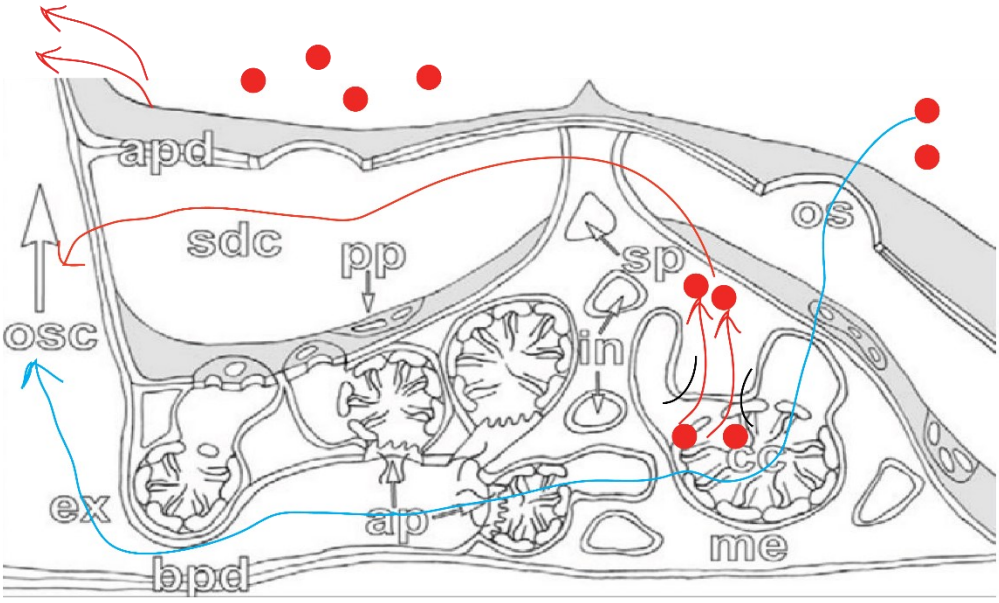
apd
sdc
pp
sp
os
osc
in
cc
ex
ap
me
bpd

Figure 3: Visual summary of possible routes of L-glutamate movement through the sponge, adapted from Elliott and Leys 2007. L-glutamate (red spheres) may enter through normal flow through the sponge (blue arrow) and then move into the mesohyl space around the sponge and then diffuse to the osculum (osc, interior red arrows). Alternatively, L-glutamate may be transported directly across the surface of the osculum into the mesohyl where the mGluRs are most likely located (upper red arrows).

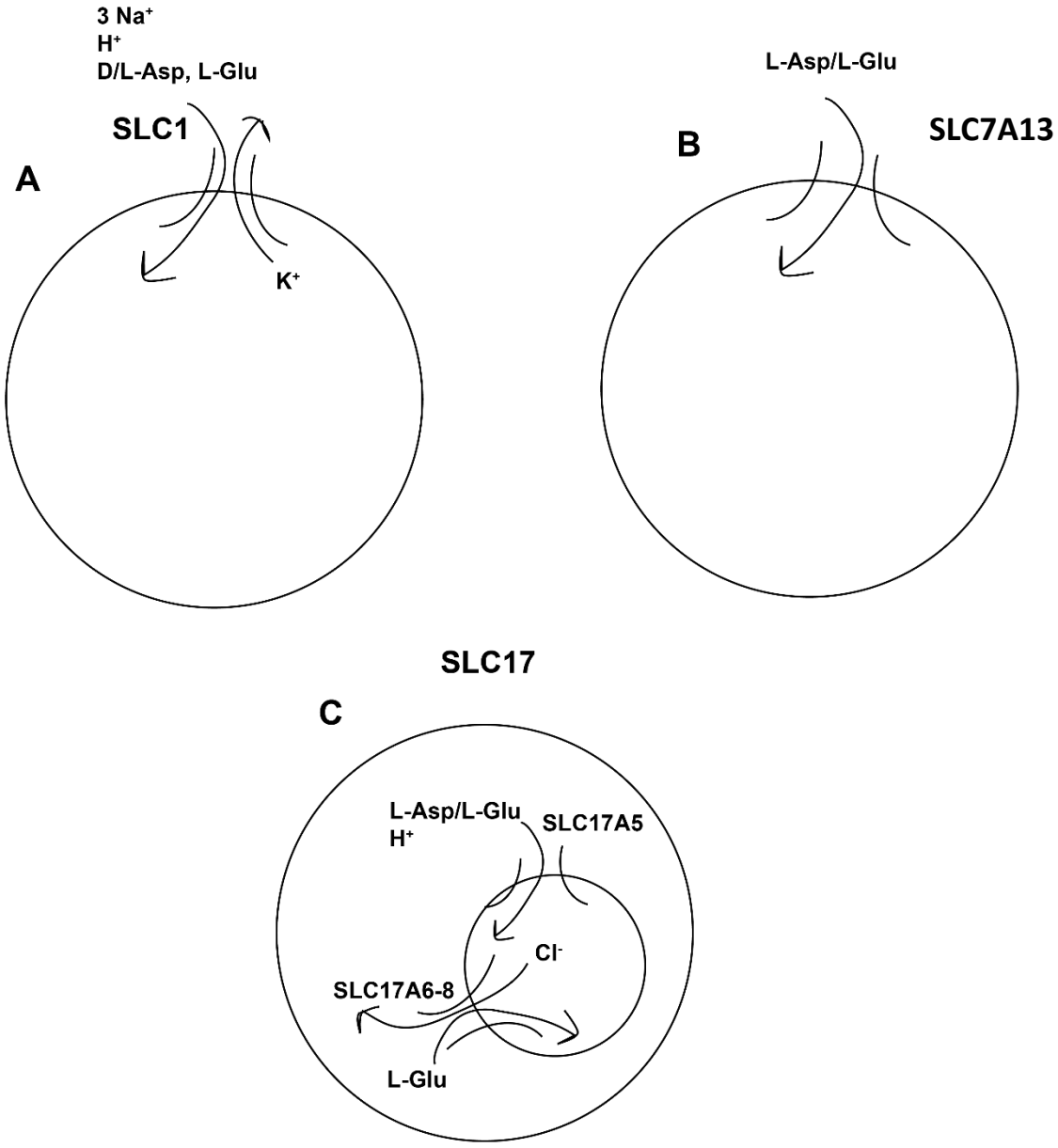
3 Na+
H+
D/L-Asp, L-Glu
SLC1
A
K+
L-Asp/L-Glu
B
SLC7A13
SLC17
C
L-Asp/L-Glu
H+
SLC17A5
Cl-
SLC17A6-8
L-Glu

Figure 4: Localization and ion dependencies of L-glutamate transporters. Visual representation of data contained within Table 2. A: SLC1 transporters balance the movement of one potassium ion out of the cell with the movement of 3 sodium ions, a proton, and a molecule of either L-glutamate or L-aspartate. B: SLC7A13 has an unknown mechanism of action, and transports both L-aspartate and L-glutamate across the cell membrane. C: SLC17A5 couples movement of L-glutamate or L-aspartate into a vesicle with movement of a proton. SLC17A6-8 (VGLUT) instead couple movement of L-glutamate into the vesicle with movement of chloride out of the vesicle.

2. Materials and Methods:

2.1 Sponge culture:

Ephydatia muelleri tissue containing gemmules was collected by S. Leys from both the head tank of the Victoria Capital Regional District water system in 2017 and O'Connor Lake in 2018 and brought back to the University of Alberta, Edmonton AB where they were kept at 4°C. Sponge gemmules were cultured as outlined in (Leys et al. 2019a). Gemmules are asexually produced genetically identical progeny of sponges that are resistant to environmental pressures including extended freezing and anoxia (Ungemach et al. 1997, Reiswig and Miller 1998). Gemmules were removed from the spicule skeleton using gentle pressure over a corduroy surface and washed with 1% H_2O_2 for five minutes. To hatch, gemmules were transferred to 6 well cell culture plates (Corning Costar, Kennebunk, ME, USA) containing either Strekal's medium (0.9 mM $MgSO_4$ • 7 H_2O, 0.5 mM $CaCO_3$, 0.1 mM Na_2SiO_3• 9 H_2O, 0.1 mM KCl, pH 6.8)(Strekal and McDiffett 1974) or M-medium (0.5 mM $MgSO_4$ • 7 H_2O, 1 mM $CaCl_2$ • 2 H_2O, 0.5 mM $NaHCO_3$, 0.05 mM KCl, 0.25 mM Na_2SiO_3)(Rasmont 1961)(Table 1). M-medium was used for inulin, time series, and concentration series experiments (see below). Strekal's medium was used in later experiments due to greater ease of ion substitution. Sponge media was changed every two days after gemmules hatched. Sponges with a fully developed aquiferous system (7-10 dph (days post hatching), stage 5) were used for all experiments. Empty gemmule husks were removed from the cultures to reduce the influence of the gemmule husk on protein content assays, and sponges were allowed to heal for 16 hours. After 16 hours the media was replaced (3

mL total determined gravimetrically). Sponges were allowed to rest undisturbed for another 16 hours prior to the start of experiments.

2.2 Inulin uptake experiments:

To determine if L-glutamate uptake was due to diffusion or specific uptake, either 0.1 μCi ^{14}C-inulin (Perkin Elmer, Boston, MA, USA) or 0.3 μCi ^{14}C-L-glutamate (Moravek, Brea, CA, USA) in 30 μM total L-glutamate was added to each well with sponges. Experimental incubations lasted for either 30 minutes or 24 hours. Water samples (50 μL) were taken in triplicate from each well at t=0 and after t=30 minutes or 24 hrs and kept at RT until analyzed for radioactivity. Each well with sponges was washed 3 times with either 1 mM inulin or 100 μM L-glutamate for five minutes each to remove loosely bound label. Three 50 μL water samples were taken after each wash and stored as above. Sponge tissue was removed from the well using a 25 cm handle cell scraper (Fisher Scientific, Ottawa, ON) and transferred by micropipette into a 1.5 mL Eppendorf tube containing 1% w/v sodium dodecyl sulfate (SDS) (Fischer Scientific) and incubated at 60 °C for 16 hours. Tissue samples were homogenized in 1% SDS using a handheld microtube tissue homogenizer (Fischer Scientific) and three 25 μL samples of homogenized tissue were transferred to Eppendorf tubes and stored at RT for radioisotope analysis.

2.3 Radioisotope analysis and protein analysis:

To quantify the amount of radiolabeled L-glutamate that was taken up by sponges, 1 mL of Optiphase Hisafe 3.0 (Perkin Elmer) was added to each 50 μL water sample. For homogenized tissue samples, 1 mL of Ultima Gold AB scintillation fluor (Perkin Elmer) was added to each 25 μL sample. The amount of scintillation fluor used ensured sufficient scintillant was available for all decay events in the sample to be visible during counting. Samples were

placed in the dark for 2 hours to quench possible autofluorescence and counted for five minutes each using a Beckman LS 6000TA beta counter. Protein content of sponge samples was determined using the microplate protocol of a Pierce BCA assay kit (Thermo Scientific) against a standard curve composed of 0-1.5 mg mL^{-1} of bovine serum albumin (BSA) (Thermo Scientific). On average each sponge gemmule added 9.76 µg of protein to each sponge (Figure 5).

Uptake rate into the sponge tissue (J, picomol/minute) was determined by using the specific activity of the isotope (SA, 281 mCi/mmol), counts per minute of the sample (CPM), divided by the incubation time in minutes (T) using the following formula:

$$J = CPM/SA * 1/T$$

Uptake rates were normalized to the amount of protein in each sample.

2.4 Glutamate uptake time series experiments:

To determine if L-glutamate uptake was variable over different time scales, glutamate uptake rate was determined by measuring uptake after 0.5, 2, 4, 6, 8, 16, or 24 hr incubation in 0.3 µCi ^{14}C-L-glutamate and 30 µM total L-glutamate. All water and tissue samples taken, and washes were carried out as above (Section 2.2).

2.5 Concentration dependent uptake kinetics:

To characterize the K_m and J_{max} of putative transporters, glutamate uptake rate was determined by measuring uptake of radiolabeled L-glutamate at 0, 1, 3, 6, 9, 10, 15, 20 or 30 µM over 16 hrs. The amount of isotope used for each sponge was changed ratiometrically with total glutamate concentration at a ratio of 0.1 µCi ^{14}C-L-glutamate / 10 µM L-glutamate. All water and tissue samples taken, and washes were carried out as above (Section 2.2).

2.6 Competition experiments:

To determine the specificity of the putative transporters, D-glutamate, L-aspartate, and L-alanine were applied at a ratio of 2:1 (12 μM) or 10:1 (60 μM) to unlabeled L-glutamate. A ratio of 0.1 μCi ^{14}C-L-glutamate / 10 μM L-glutamate was used as previously (Section 2.5), at a total L-glutamate concentration of 6 μM. An incubation period of 16 hours was used for all trials. Controls without the addition of other amino acids were run in parallel to experimental groups. All other steps were carried out as described previously.

2.7 Ion substitution experiments:

All containers used to store ion substituted media were pre-treated with 0.1% trace metals basis nitric acid for 24 hours to minimize excess ion contamination. Reduced sodium Strekal's medium was prepared by substituting Na_2SiO_3 with 0.1 mM N-methyl D-glucamine (NMDG) conjugated silicic acid. Reduced calcium Strekal's medium was prepared without $CaCO_3$ and by exposing the medium to air to equilibrate carbonic acid concentrations. Reduced sodium and calcium medium was made by substituting Na_2SiO_3 with NMDG conjugated silicic acid and without $CaCO_3$. Unmodified Strekal's medium was removed using nitric acid-soaked glass pipettes (Fisher Scientific) and replaced with sodium and/or calcium reduced medium containing 0.06 μCi ^{14}C-L-glutamate to 6 μM L-glutamate. Sponges were incubated in ion-reduced media for 6 hours. Control sponges in normal medium were run in parallel with experimental groups. All other steps were carried out as described previously.

2.8 Modified pH experiments:

Strekal's medium buffered to pH 8.5 using 5 mM Tris base (Fischer Scientific) was used to test the effect of increased pH on L-glutamate uptake. Bafilomycin A1 (100 nM) was added to normal Strekal's medium (pH 6.8) to test proton dependence of uptake. Experiments were carried out using a ratio of 0.06 μCi to 6 μM L-glutamate and an incubation time of 6 hours. All other steps were carried out as described previously.

2.9 Homology searches

To determine the complement of L-glutamate transporters within the *E. muelleri* genome, *E. muelleri* sequences were extracted from a database of transcribed genomic sequences using human sequences gathered from the NCBI protein database as the query. Mammalian sequences were used as queries due to evaluation of the functional properties of the transporters having been performed in these systems (reviewed in Kanai et al. 2013, Reimer 2013). Sequence matches with an expectation value (e-value) less than e^{-20} were further analyzed. Identity of individual sequences was confirmed through reciprocal BLAST against the non-redundant(nr) protein database with an e-value cutoff of e^{-20} (Altschul et al. 1990). Genes from solute carrier (SLC) families 1,3,7,8, and 17 were used for the analysis, as well as organisms sampling the diversity of metazoans: *Homo sapiens, Mus musculus, Danio rerio, Nematostella vectensis, Capitella teleta, Saccoglossus kowalevskii, Aplysia californica,* and *Daphnia pulex*. All other SLC transporters used within the phylogeny were sourced within the NCBI protein database and confirmed using reciprocal BLAST with human sequences.

2.10 Phylogenetic analysis

Sequences were aligned using MAFFT with the alignment strategy set to Auto and using default parameters (Katoh et al. 2019). This alignment was then automatically trimmed using TrimAl version 1.3 using the Automated 1 method (Capella-Gutierrez et al. 2009). A maximum likelihood tree was computed using MEGA7 with 100 bootstrap replicates using the Jones-Taylor-Thornton model of sequence evolution (Jones et al. 1992, Kumar et al. 2016). Settings were otherwise set to their defaults, and MEGA was used due to familiarity with the program.

2.11 Statistical analysis:

Concentration dependent L-glutamate uptake was plotted in SigmaPlot version 13.0 (Systat Software, San José, CA, USA) using iterative curve fitting. The data was fitted to a sigmoidal curve with the following equation:

$$y = \frac{a}{1 + e^{(-x - \frac{x_o}{b})}}$$

Where x is the glutamate concentration, a is the maximal rate of transport (J_{max}), and x_o is the glutamate concentration at which half of maximum transport is achieved (K_m). The kinetic parameters of putative transporters were also independently evaluated through use of Lineweaver-Burk plots. Statistical comparisons involving 3 groups or more were carried out using one-way analysis of variance (ANOVA) with a Holm-Sidak post hoc test to confirm significance between pairs of treatments. All comparisons between 2 groups were performed using a one-tailed t-test for normal data or a Mann-Whitney test for non-normal data. Outliers in data sets were detected using a Grubbs test with a significance value of 0.05. A Mann-Whitney test was only run if the data could not be log transformed to be normal. All data are expressed as

mean ± standard error of the mean (S.E.M) and a significance value of 0.05 was used for all tests.

2.12 Source of Reagents:

All chemicals were obtained from Sigma-Aldrich unless otherwise indicated.

Ion	M-medium	Strekal's medium
Mg^{2+}	500 µM	900 µM
SO_4^{2-}	500 µM	900 µM
Ca^{2+}	1 mM	500 µM
CO_3^{2-}	0 µM	500 µM
HCO_3^-	500 µM	0 µM
Na^+	1 mM	200 µM
SiO_3^{2-}	250 µM	100 µM
K^+	50 µM	100 µM
Cl^-	2.05 mM	100 µM
Total osmolarity	5.85 mOsm/L	3.3 mOsm/L

Table 1: Comparison of ionic content of M-media and Strekal's media (Rasmont 1961, Strekal and McDiffet 1974). Total osmolarity is calculated as a sum of the total ionic content of the media.

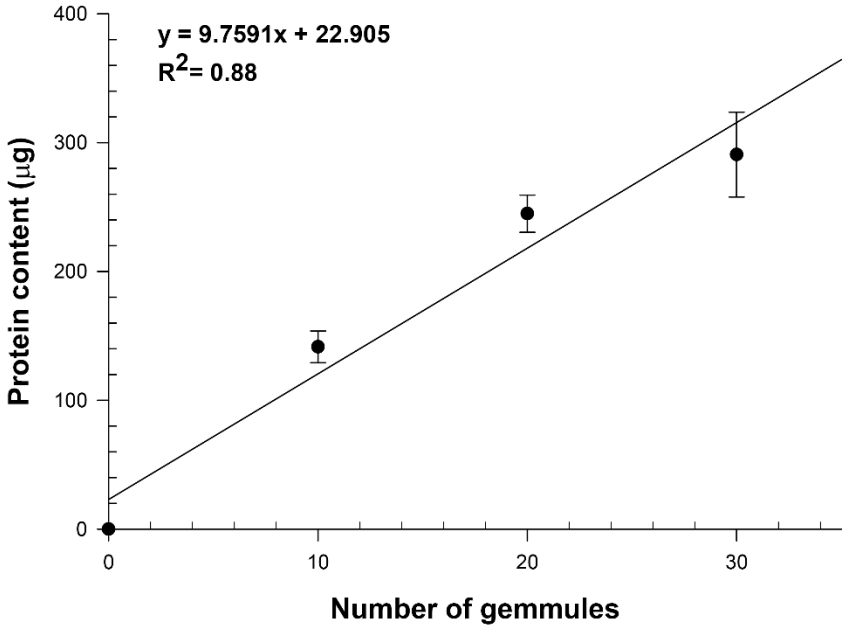
y = 9.7591x + 22.905
R2= 0.88
Protein content (µg)
Number of gemmules
400
300
200
100
0
0
10
20
30

Figure 5: Average protein content per gemmule for *E. muelleri*. Protein concentration was determined using BCA assay, values represent the mean ± S.E.M. of 4 individual sponges.

3. Results:

3.1 Uptake kinetics:

Experiments comparing the rate of uptake of the large sugar polymer inulin with that of L-glutamate were performed to determine the relative contribution of diffusion to the total uptake of L-glutamate by *Ephydatia*. Uptake of 30 μM total L-glutamate across *E. muelleri* was 30-fold greater than 0.1 μCi inulin after a 30 min incubation period ($p < 0.01$) (Figure 6A). This difference in uptake became more pronounced after a 24 hour incubation period, with uptake of L-glutamate being more than 600-fold greater than the uptake of inulin ($p < 0.01$) (Figure 6B). The large difference between uptake of inulin and L-glutamate suggests that a transport process(either facilitated diffusion or active transport) is being used for L-glutamate uptake. This also supports that the wash protocol used following the incubation period with the radioisotope is effectively preventing any isotope from being trapped within the aquiferous system of the sponge.

Comparisons of the uptake rate of L-glutamate over different total incubation periods were performed to determine a sufficent incubation period for readily detectable L-glutamate uptake. Uptake of 30 μM total L-glutamate over varying incubation periods (0.5,2,4,6,8,16, 24 hrs) did not show a clear trend over time, with the largest differential being a 3-fold greater uptake rate after a 24-hour incubation compared to a 16 hour incubation ($p < 0.01$) (Figure C). A sixteen hour incubation time frame was chosen for future experiments so that during scintillation counting the 1 μM L-glutamate exposed samples would have counts per minute of at least 100 to reduce error in measurement.

Subsequently, L-glutamate uptake rate over a range of concentrations was determined to identify concentrations at which putative transporters may be acting. Uptake of L-glutamate across *E. muelleri* was characterized by two concentration dependent curves (0,1,3,6,9,10,15,20,30 µM total L-glutamate) (Figure 7A,B). At low concentrations (below 10 µM) there was a sigmoidal relationship between uptake rate and substerate concentration. This curve displayed an uptake capacity of J_{max} = 25.1 ± 1.71 pmols mg^{-1} min^{-1} and a substrate concentration giving 50% of maximal uptake at 2.87 ± 0.35 µM (R^2 = 0.69) (Figure 7A). Gradual increase in uptake of L-glutamate was observed over substrate concentrations of L-glutamate ranging from 0 µM to 60 µM. This followed a linear fit overall (R^2 = 0.78), with a weaker sigmoidal fit at concentrations below 30 µM with a period of exponential increase in uptake rate with L-glutamate concentration followed by a plateau at larger concentrations (J_{max} = 64.24 ± 4.7 pmols mg^{-1} min^{-1}, K_m = 8.77 ± 0.84 µM, R^2 = 0.65) (Figure 7B). Lineweaver-Burk analysis of L-glutamate uptake found a J_{max} of 43.48 pmol L-glutamate mg^{-1} min^{-1} and a K_m of 21.73 µM for the putative transporter acting between L-glutamate concentrations of 0-30 µM, and for the putative transporter acting at concentrations below 10 µM a J_{max} of 25.64 pmols L-glutamate mg^{-1} min^{-1} and a K_m of 13.54 µM. The close overlap of the different estimated kinetic parameters of the transporters thus complicates conclusions that can be drawn, as well as the difference between the Linewaever-Burk estimates and the sigmoidal curve fit estimates.

3.2 Inhibition and ion dependence:

Experiments involving application of other amino acids to sponges during L-glutamate uptake were performed in order to gain insight into other potential substrates of putative transporters. Negatively charged amino acids (D-glutamate and L-aspartate) competitively

inhibited the uptake of L-glutamate across *E. muelleri*. Application of 60 µM of the enantiomer D-glutamate in the presence of 6 µM L-glutamate led to a 2-fold reduction in uptake relative to 6 µM L-glutamate controls ($p < 0.05$) (Figure 8A). Application of 12 µM D-glutamate in the presence of 6 µM L-glutamate in contrast did not elicit a significant change in uptake ($p = 0.24$)(Figure 8A). Application of 60 µM of the other negatively charged amino acid L-aspartate in the presence of 6 µM L-glutamate led to a 3-fold reduction in uptake relative to 6 µM L-glutamate controls($p < 0.05$) while application of 12 µM L-aspartate in the presence of 6 µM L-glutamate did not elicit a significant change in uptake ($p = 0.11$) (Figure 8B). These results suggest that L-aspartate and D-glutamate are either taken up by the sponge or that the transporters used by the sponge are competitively inhibited by other negatively charged amino acids.

In contrast, application of both 60 µM ($p = 0.08$) and 12 µM ($p = 0.61$) of the neutral amino acid L-alanine in the presence of 6 µM L-glutamate did not lead to significant changes in uptake relative to 6 µM L-glutamate controls in one experiment, but in a replicate experiment both 12 µM and 60 µM significantly reduced L-glutamate uptake (Figure 8C, S1). This suggests that L-glutamate uptake in *Ephydatia* might be tied to a more general amino acid acquisition mechanism.

Substitution of media components was performed in order to attempt to determine if an ionic gradient is necessary for L-glutamate uptake by *E. muelleri*. Uptake rate of L-glutamate in media with N-methyl D-glucamine substituted for sodium was not significantly different from 6 µM L-glutamate controls, with different experiments indicating no difference, reduced uptake, and increased uptake (Figure 9A, S2A). The uptake rate of L-glutamate in media with calcium excluded and either with or without the chelator EGTA was also not significantly different from

6 µM L-glutamate controls (Figure 9B, S2B). However, the uptake rate of L-glutamate in media that is reduced in both sodium and calcium was 30% lower than unaltered media controls in one experiment and 30% higher in another, which was significantly different in both cases ($p < 0.05$) (Figure 9C, S2C). Overall uptake rates in this experiment were lower in general than other experiments, including in the controls. High variability in experiments with ion substituted media thus prevents a clear conclusion being reached on the role of ions in L-glutamate uptake.

Finally, modifications to the proton content of media were assayed to determine if changes in pH may serve as a driving gradient for L-glutamate uptake. L-glutamate uptake was also not affected by alteration of media pH. Increasing the pH of the *E. muelleri* media from 6.8 to 8.5 did not lead to signficant changes in L-glutamate uptake ($p = 0.91$) (Figure 10A). Application of a proton ATPase inhbitor, 100 nM bafilomycin, showed no change in uptake rates of L-glutamate ($p = 0.8$) (Figure 10B). These results suggest that L-glutamate uptake in *E. muelleri* is not proton dependent.

3.3 *E. muelleri* L-glutamate transporter complement:

Examination of the genome of *E. muelleri* for SLC transporters involved in L-glutamate transport was done to contextualize the transport properties seen in previous experimental work. Ten total L-glutamate transporters were found in the *E. muelleri* genome (Figure 11). Two of these transporters group with the SLC1 family of transporters. Comparison of an alignment of the two sequences with the human and mouse SLC1A3 sequences shows that the two *E. muelleri* sequences are identical in their amino acid sequence (Figure 12). Additionally, the *E. muelleri* sequences are only 205 amino acids compared to the 543 and 542 amino acids found in the human and mouse SLC1A3 sequences, respectively (Table S1). The large discrepancy in size

between the sponge and mammalian sequences suggests that the sponge homologs may not be functional in L-glutamate transport.

The other eight transporters group with SLC17A5-8, which consists of sialin and the vesicular glutamate transporters (Figure 11). Aligning the *E. muelleri* sequences with the human and mouse SLC17A5 and SLC17A7 genes shows that based on sequence the 8 proteins split into four groups of two (Figure 13). Three of these groups consist of pairs of proteins that are identical to each other: Em0617g8a and Em0438g9a, Em0617g9a and Em0438g10a, and the pair of Em0074g14a and Em0005g1679a. Additionally, the two pairs of Em0617g8a and Em0438g9a plus Em0074g14a and Em0005g1679a are different from each other only be a single amino acid deletion in the Em0074g14a pair (Figure 12). The final pair of sequences, Em0074g13a and Em0005g1680a, are nearly identical except for their C termini. Most of the *E. muelleri* sequences are comparable in length to the mammalian sequences (*Ephydatia* sequences above 400 amino acids, mammalian sialin around 500 amino acids, vesicular glutamate transporters around 550 amino acids) (Table S1). However, Em0617g9a and Em0438g10a are less than 200 amino acids long, suggesting they may be nonfunctional.

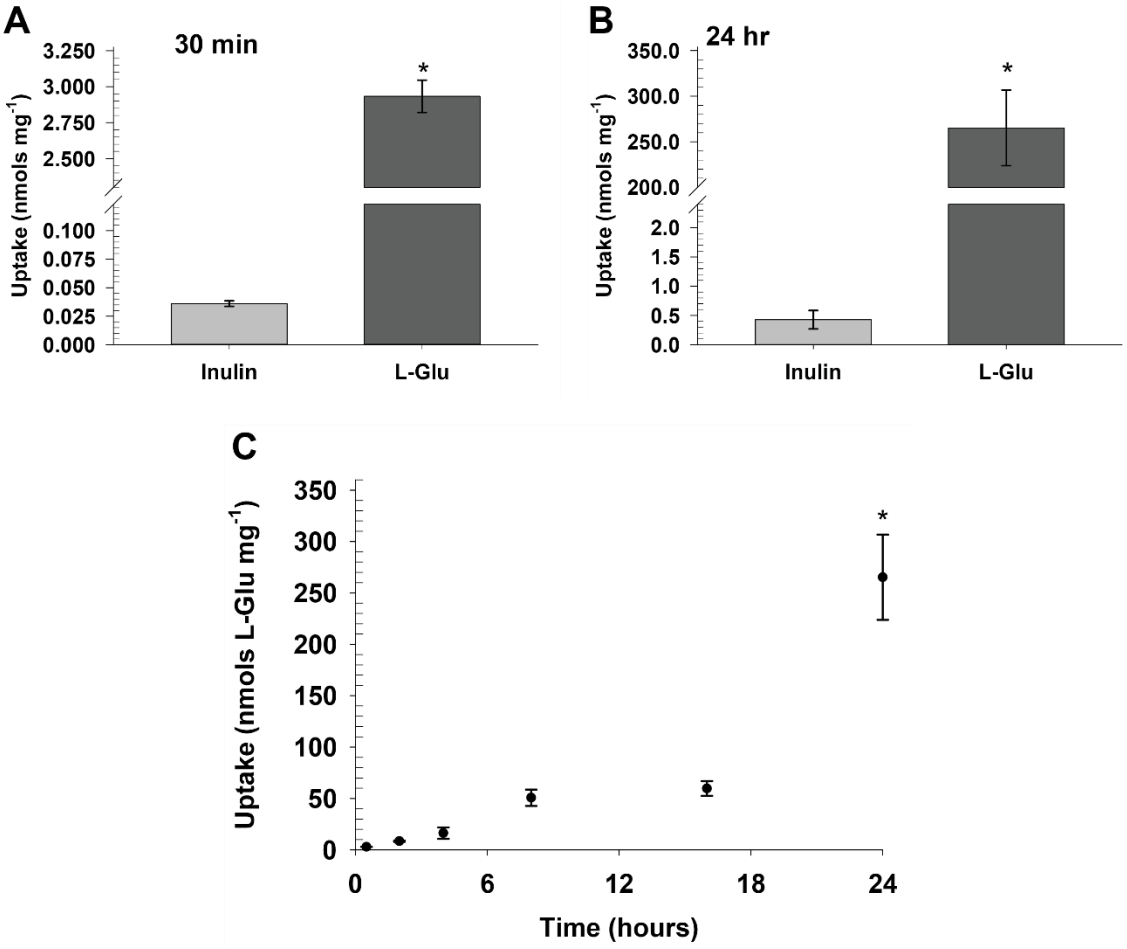
A
30 min
Uptake (nmols mg-1)
3.250
3.000
2.750
2.500
0.100
0.075
0.050
0.025
0.000
*
Inulin
L-Glu
B
24 hr
Uptake (nmols mg-1)
350.0
300.0
250.0
200.0
2.0
1.5
1.0
0.5
0.0
*
Inulin
L-Glu
C
Uptake (nmols L-Glu mg-1)
350
300
250
200
150
100
50
0
*
0
6
12
18
24
Time (hours)

Figure 6: Uptake of of 30 μM total L-glutamate across the whole body of *E. muelleri*. (A) Uptake of L-glutamate compared to inulin after a 30-minute incubation period. (B) Uptake of L-glutamate compared to inulin after a 24-hour incubation period. (C) Uptake of L-glutamate after incubation periods ranging from 30 minutes to 24 hours. Values represent the mean ± standard error of the mean (S.E.M) of 3-5 replicates. Asterisks denote a significant difference between treatments as assessed by a two tailed t-test at $\alpha = 0.05$.

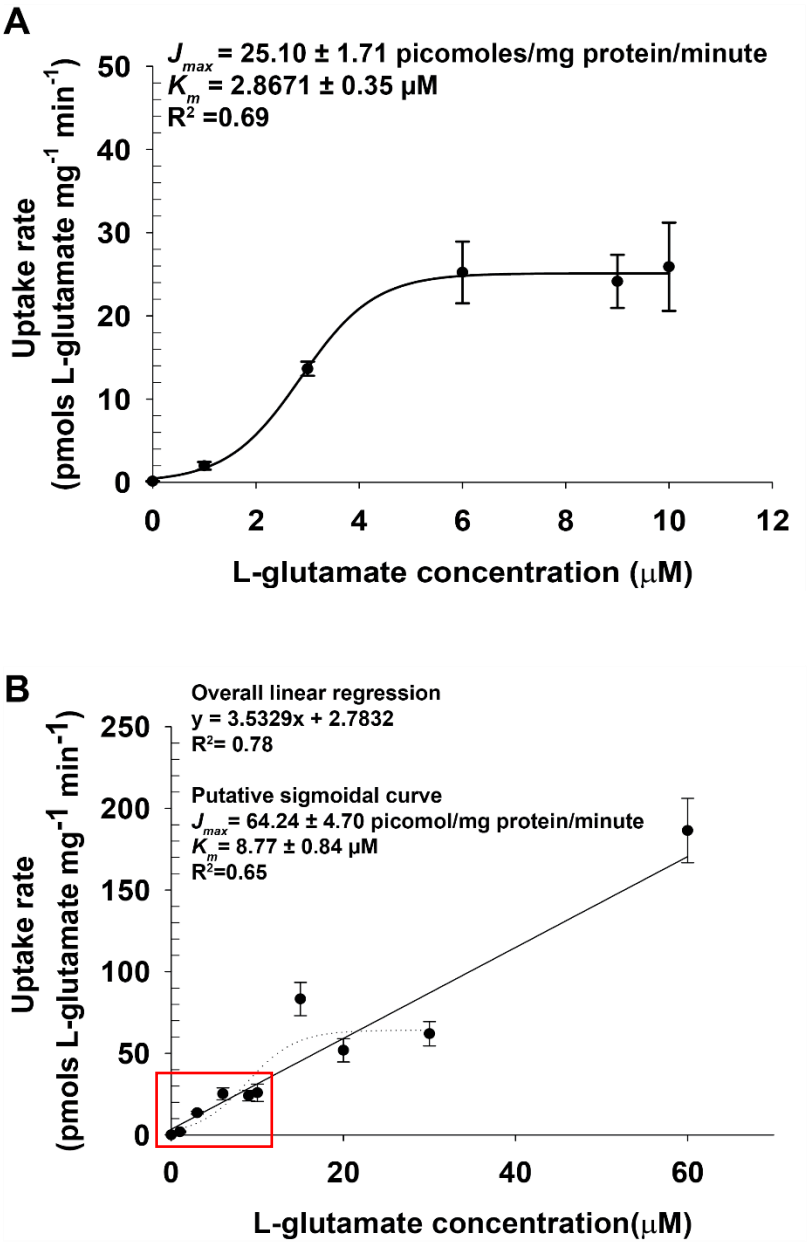
A
J_{max} = 25.10 ± 1.71 picomoles/mg protein/minute
K_m = 2.8671 ± 0.35 µM
R^2 =0.69
Uptake rate
(pmols L-glutamate mg^{-1} min^{-1})
0
10
20
30
40
50
0
2
4
6
8
10
12
L-glutamate concentration (µM)
B
Overall linear regression
y = 3.5329x + 2.7832
R^2= 0.78
Putative sigmoidal curve
J_{max}= 64.24 ± 4.70 picomol/mg protein/minute
K_m= 8.77 ± 0.84 µM
R^2=0.65
Uptake rate
(pmols L-glutamate mg^{-1} min^{-1})
0
50
100
150
200
250
0
20
40
60
L-glutamate concentration(µM)

Figure 7: Uptake of L-glutamate across the body of *E. muelleri* in 16 hours across increasing concentrations of L-glutamate ranging from 0 μM to 60 μM. (A) Concentration curve for concentrations of L-glutamate ranging between 0-10 μM. (B) Concentration curve for concentrations of L-glutamate ranging between 0-60 μM. The region in the red box corresponds to the curve shown in part A. Values represent the mean ± standard error of the mean (S.E.M) of 4-9 replicates.

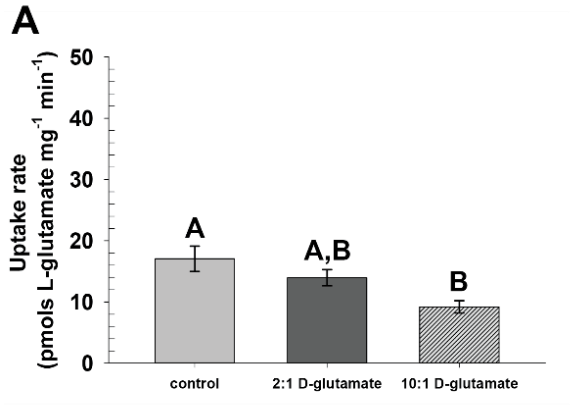
A
Uptake rate (pmols L-glutamate mg-1 min-1)
50
40
30
20
10
0
A
A,B
B
control
2:1 D-glutamate
10:1 D-glutamate

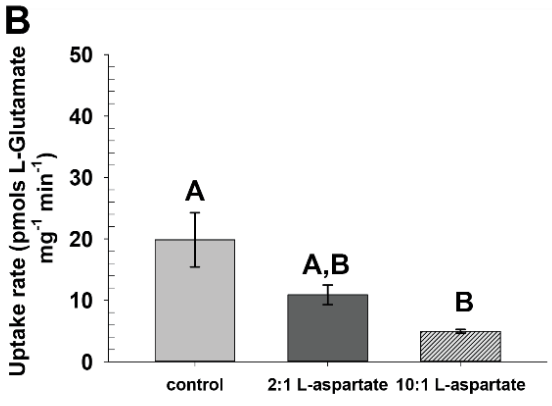
B
Uptake rate (pmols L-Glutamate mg-1 min-1)
50
40
30
20
10
0
A
A,B
B
control
2:1 L-aspartate
10:1 L-aspartate

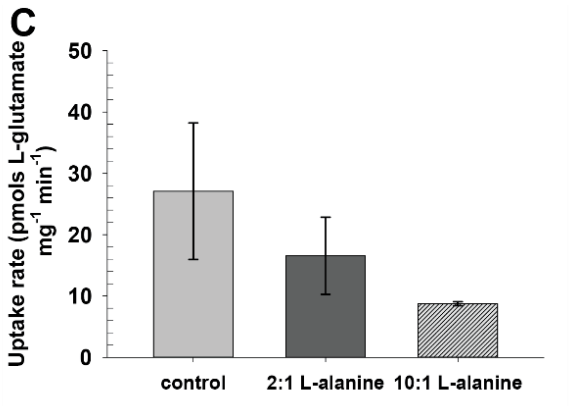
C
Uptake rate (pmols L-glutamate mg-1 min-1)
50
40
30
20
10
0
control
2:1 L-alanine
10:1 L-alanine

Figure 8: Uptake of 0.06 μCi ^{14}C-L-glutamate in 6 μM total L-glutamate across the body of *E. muelleri* in the presence of other amino acids. A: Uptake of L-glutamate in the presence of 2:1 and 10:1 ratios of D-glutamate. B: Uptake of L-glutamate in the presence of 2:1 and 10:1 ratios of L-aspartate. C: Uptake of L-glutamate in the presence of 2:1 and 10:1 ratios of L-alanine. All incubation periods were 16 hours. Values represent the mean ± standard error of the mean (S.E.M) of 5-6 replicates. Similar letters denote no significant difference between treatments, letters that are different indicate significant differences between treatments as determined by one-way ANOVA with Holm-Sidak post hoc tests at $\alpha = 0.05$.

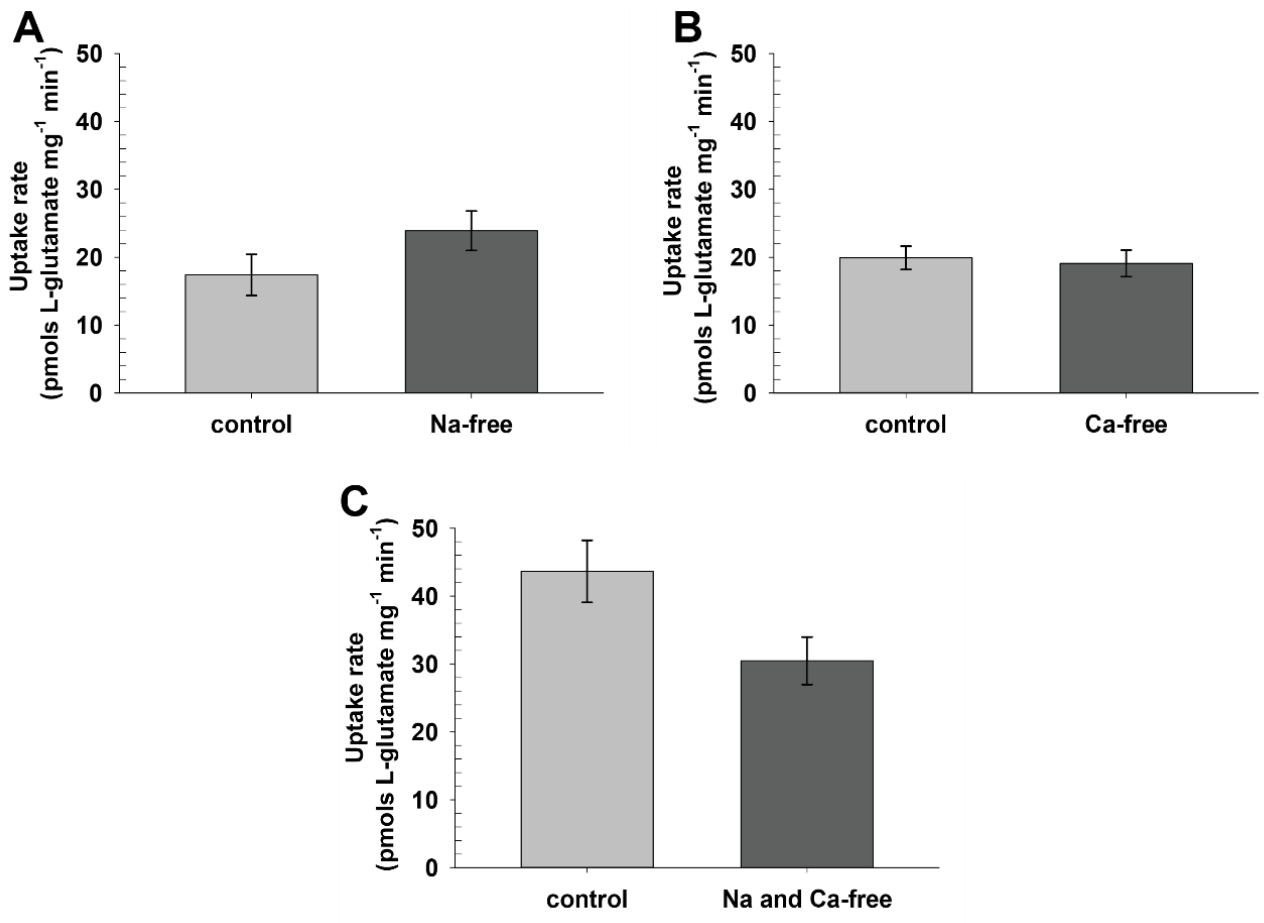
A
Uptake rate
(pmols L-glutamate mg-1 min-1)
50
40
30
20
10
0
control
Na-free
B
Uptake rate
(pmols L-glutamate mg-1 min-1)
50
40
30
20
10
0
control
Ca-free
C
Uptake rate
(pmols L-glutamate mg-1 min-1)
50
40
30
20
10
0
control
Na and Ca-free

Figure 9: Uptake of 0.06 μCi ^{14}C-L-glutamate in 6 μM total L-glutamate across the body of *E. muelleri* with a reduction of sodium and/or calcium. A: Uptake of L-glutamate in media with N-methyl D-glucamine substituted for sodium. B: Uptake of L-glutamate in media with calcium excluded. C: Uptake of L-glutamate in media reduced in both sodium and calcium. All incubation periods were 6 hours. Values indicate the mean ± standard error of the mean (S.E.M) of 9 replicates. Asterisks denote a significant difference between treatments as assessed by a two-tailed t-test at $\alpha = 0.05$.

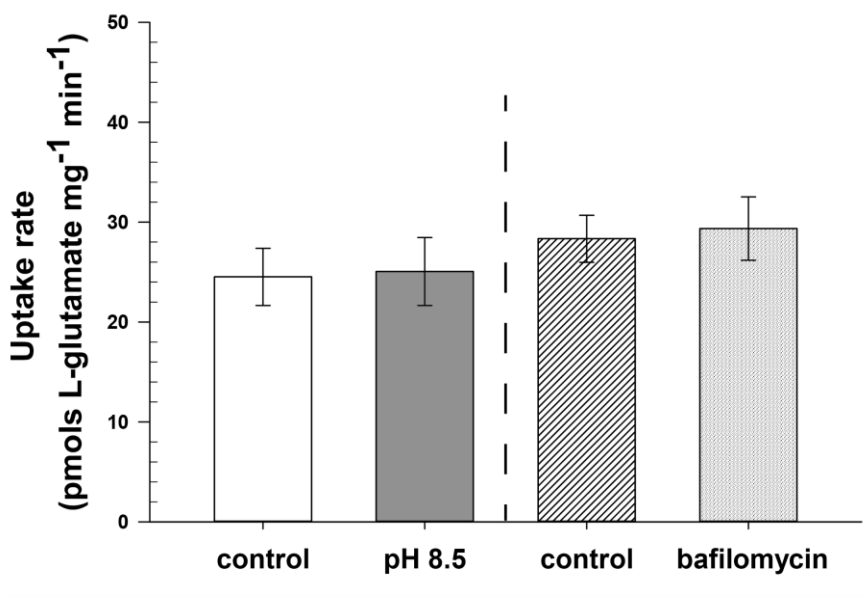
Uptake rate
(pmols L-glutamate mg-1 min-1)
50
40
30
20
10
0
control
pH 8.5
control
bafilomycin

Figure 10: Uptake of 0.06 µCi ^{14}C-L-glutamate in 6 µM total L-glutamate across the body of *E. muelleri* in basic conditions and in the presence of the proton ATPase inhibitor bafilomycin. A: Uptake of L-glutamate in standard media (pH 6.8) and pH 8.5 media. B: Uptake of L-glutamate in the presence of bafilomycin. All incubation periods were 6 hours. Values represent the mean ± standard error of the mean (S.E.M) of 6-9 replicates.

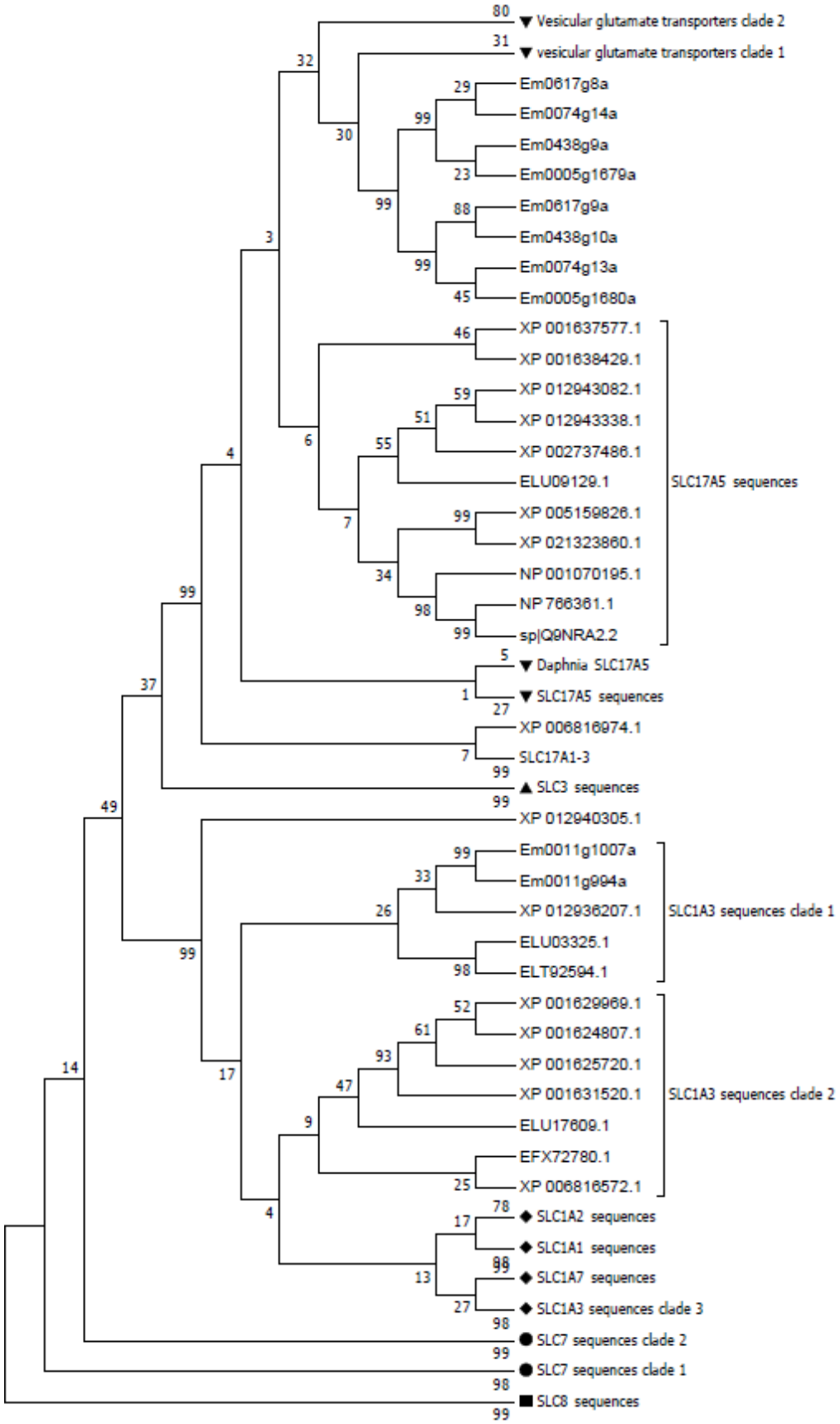
Vesicular glutamate transporters clade 2
vesicular glutamate transporters clade 1
Em0617g8a
Em0074g14a
Em0438g9a
Em0005g1679a
Em0617g9a
Em0438g10a
Em0074g13a
Em0005g1680a
XP 001637577.1
XP 001638429.1
XP 012943082.1
XP 012943338.1
XP 002737486.1
ELU09129.1
XP 005159826.1
XP 021323860.1
NP 001070195.1
NP 766361.1
sp|Q9NRA2.2
SLC17A5 sequences
Daphnia SLC17A5
SLC17A5 sequences
XP 006816974.1
SLC17A1-3
SLC3 sequences
XP 012940305.1
Em0011g1007a
Em0011g994a
XP 012936207.1
ELU03325.1
ELT92594.1
SLC1A3 sequences clade 1
XP 001629969.1
XP 001624807.1
XP 001625720.1
XP 001631520.1
ELU17609.1
EFX72780.1
XP 006816572.1
SLC1A3 sequences clade 2
SLC1A2 sequences
SLC1A1 sequences
SLC1A7 sequences
SLC1A3 sequences clade 3
SLC7 sequences clade 2
SLC7 sequences clade 1
SLC8 sequences

Figure 11: Phylogenetic positioning of L-glutamate transporters detected in the *E. muelleri* genome. A maximum likelihood heuristic was used to generate the tree with 100 bootstrap replicates. Bootstrap values are indicated at site of condensation for condensed branches or at nodes on uncondensed branches. A total of 219 sequences were used in the analysis, with alignment of sequences using MAFFT and trimming of sequences to a 271 amino acid frame done using TrimAl. Symbols at ends of branches indicate condensation of the subtree beyond that branch, with the bootstrap value listed for the subsequent node. Em = *Ephydatia muelleri*, SLC = solute carrier.

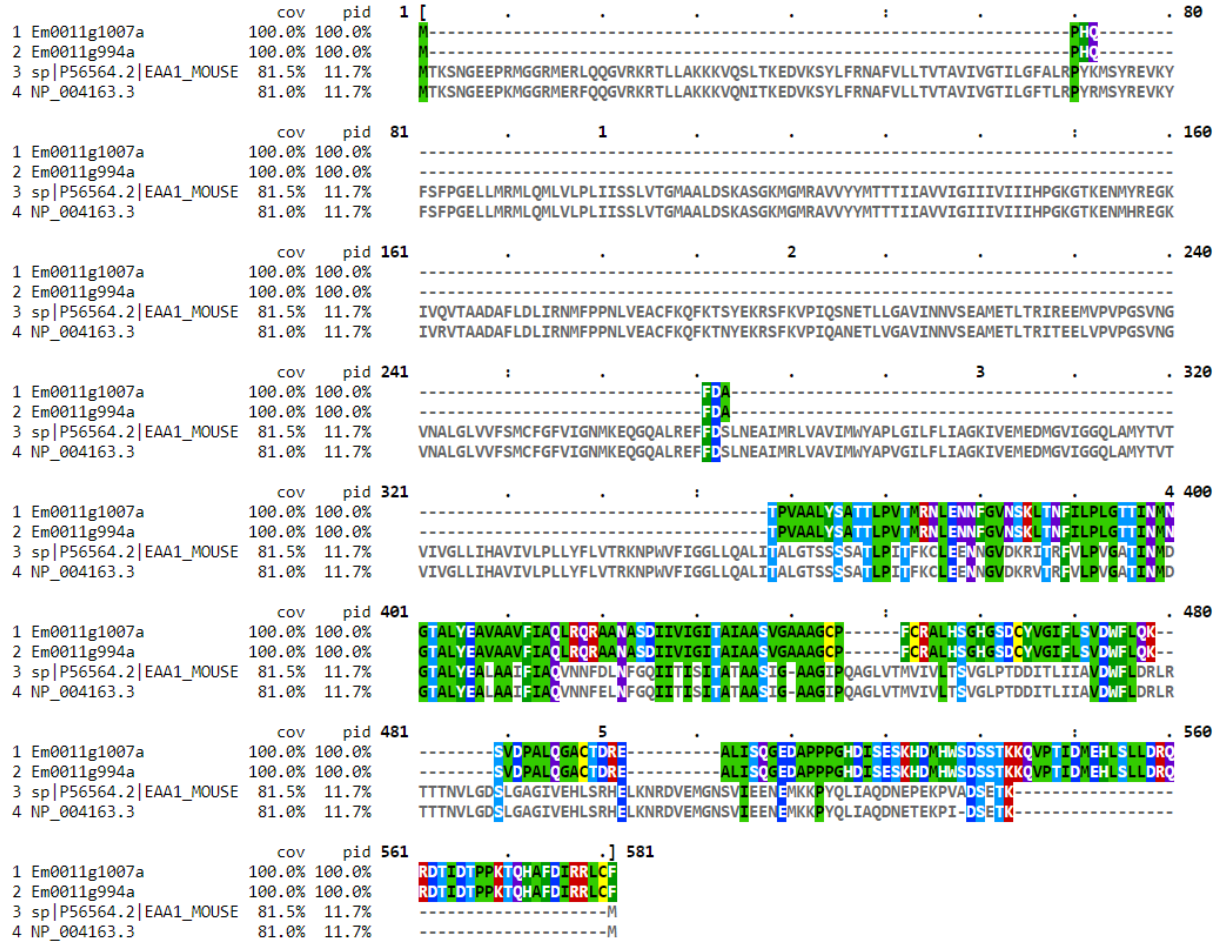
cov pid
1 Em0011g1007a 100.0% 100.0%
2 Em0011g994a 100.0% 100.0%
3 sp|P56564.2|EAA1_MOUSE 81.5% 11.7%
4 NP_004163.3 81.0% 11.7%

Figure 12: Untrimmed alignment of putative SLC1 sequences in *E. muelleri* against human and mouse SLC1A3(sequences 3 and 4). Alignment was visualized using Mview from EMBL-EBI (Madeira et al. 2019). Percent identity (pid) is compared against the first listed *E. muelleri* sequence.

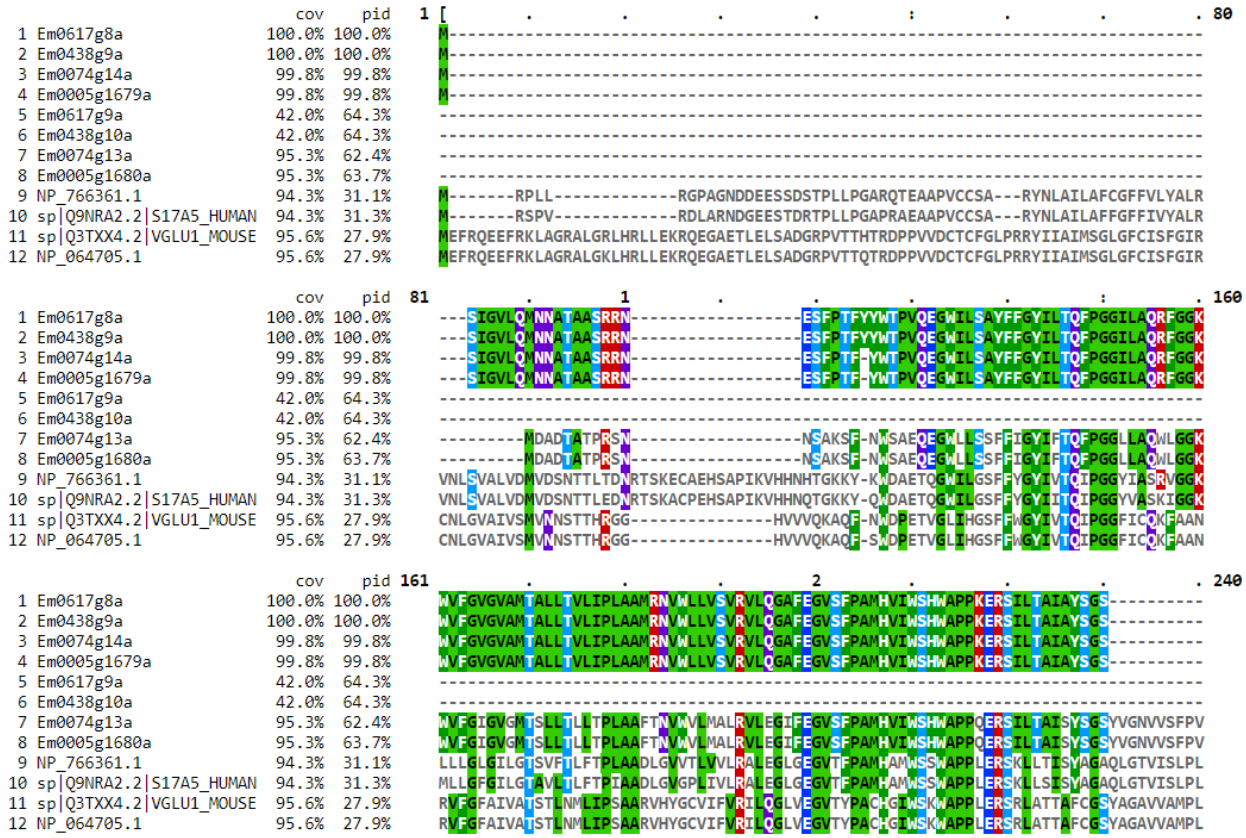
cov pid
1 Em0617g8a 100.0% 100.0%
2 Em0438g9a 100.0% 100.0%
3 Em0074g14a 99.8% 99.8%
4 Em0005g1679a 99.8% 99.8%
5 Em0617g9a 42.0% 64.3%
6 Em0438g10a 42.0% 64.3%
7 Em0074g13a 95.3% 62.4%
8 Em0005g1680a 95.3% 63.7%
9 NP_766361.1 94.3% 31.1%
10 sp|Q9NRA2.2|S17A5_HUMAN 94.3% 31.3%
11 sp|Q3TXX4.2|VGLU1_MOUSE 95.6% 27.9%
12 NP_064705.1 95.6% 27.9%

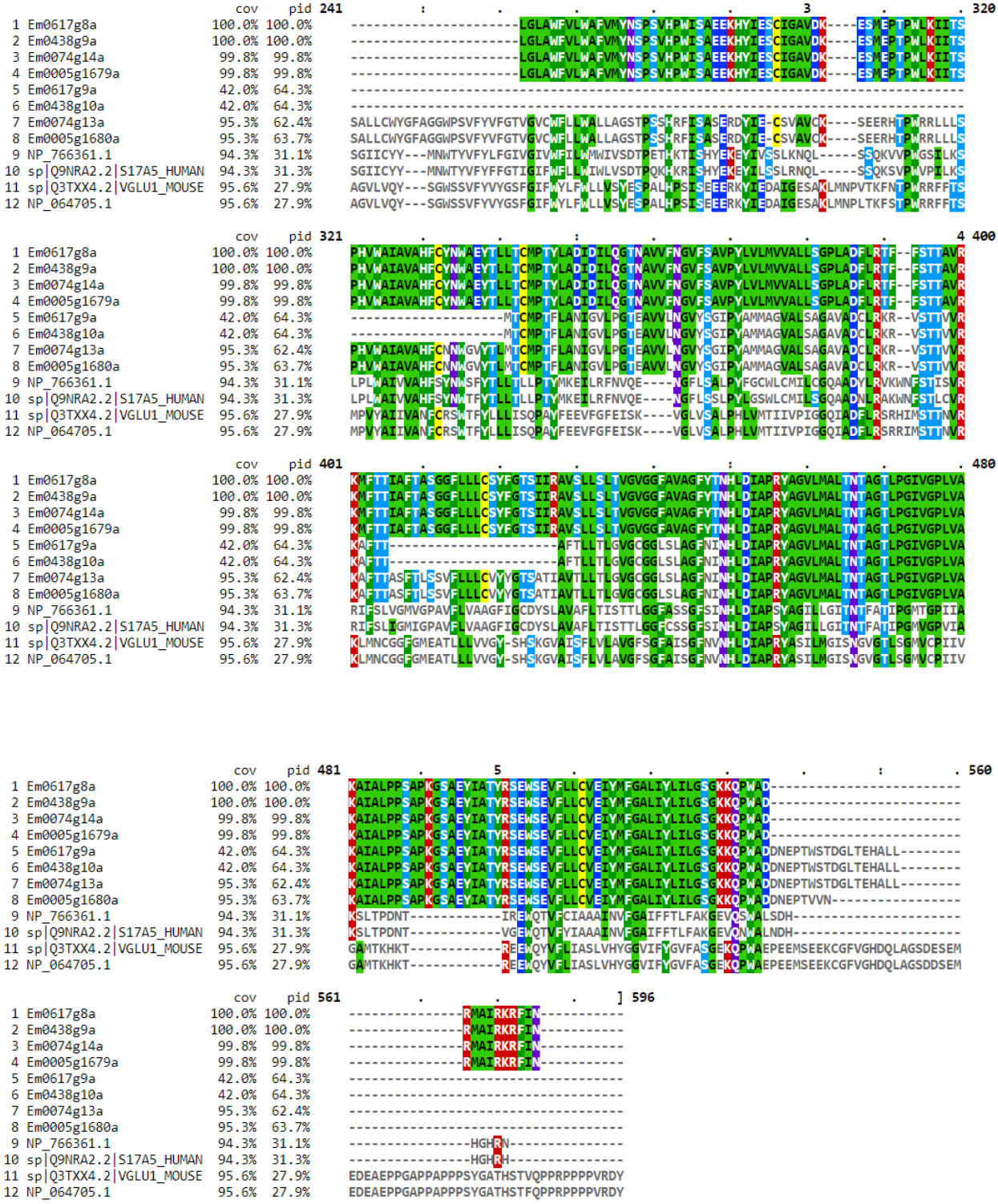
cov pid
1 Em0617g8a 100.0% 100.0%
2 Em0438g9a 100.0% 100.0%
3 Em0074g14a 99.8% 99.8%
4 Em0005g1679a 99.8% 99.8%
5 Em0617g9a 42.0% 64.3%
6 Em0438g10a 42.0% 64.3%
7 Em0074g13a 95.3% 62.4%
8 Em0005g1680a 95.3% 63.7%
9 NP_766361.1 94.3% 31.1%
10 sp|Q9NRA2.2|S17A5_HUMAN 94.3% 31.3%
11 sp|Q3TXX4.2|VGLU1_MOUSE 95.6% 27.9%
12 NP_064705.1 95.6% 27.9%

Figure 13: Untrimmed alignment of putative SLC17 sequences in *E. muelleri* against human and mouse SLC17A5(sequences 9 and 10) and SLC17A7 sequences (sequences 11 and 12). Alignment was visualized using Mview from EMBL-EBI (Madeira et al. 2019). Percent identity (pid) is compared against the first listed *E. muelleri* sequence.

4. Discussion:

This study demonstrated the specific uptake of an amino acid at very low ambient concentrations across the epithelia of the freshwater sponge *Ephydatia muelleri*. This is the first documented case of uptake of an amino acid across the extra-intestinal epithelia of a freshwater invertebrate.

4.1 Uptake Kinetics:

The uptake of L-glutamate compared to inulin in *E. muelleri* was up to 600-fold greater (Figure 6A, B). Specific transport proteins for inulin are not found in animals, so uptake of inulin into *E. muelleri* reflects solely diffusion and phagocytosis. The large discrepancy in uptake rate between L-glutamate and inulin therefore suggests that movement of L-glutamate into the body of *E. muelleri* is not solely due to diffusive mechanisms and supports the existence of a functional sealing epithelia in *E. muelleri* (Adams et al. 2010). Additionally, low concentrations of remaining inulin after procedural wash steps confirmed that the washes performed were sufficient to prevent non-bound solutes from remaining within sponges prior to tissue homogenization. The uptake rate of L-glutamate into *E. muelleri* is relatively constant for intervals up to 16 hours, with an increase in uptake rate during 24-hour incubations (Figure 6C). The stability in uptake rates over different incubation periods overall allowed for use of 16-hour incubation periods for subsequent experiments without concern for changes in uptake rates over long incubation periods.

The observed increase in L-glutamate uptake after 24 hours of incubation reflects the overall high variation between different experiments (Figure S4). Experiments run on different

days under the same manipulations can have dramatically different uptake rates. One possible source of variation in the experiments is the use of different source tissue, but generally gemmules from the same sponge individual were used for each experimental subset (Table S2). A greater possible source of variation is in manipulations made to each hatched sponge prior to experiments. Removal of gemmules from sponge tissue caused varying amounts of damage to each sponge and normalizing by protein content per sponge alone cannot reflect for possible variation due to dedication of resources to tissue repair. Differences in aggregation of gemmules into a single individual is another possible minor source of variation, with different patterns of aggregation possibly affecting media movement through the sponge and the surface area available for transport of L-glutamate.

Characterization of L-glutamate uptake in differing concentration gradients weakly supports ($R^2 = 0.65$) one transporter for L-glutamate with a Km of 8.77 μM and a J_{max} of 64.24 pmol L-Glu mg protein^{-1} min^{-1} and more strongly supports ($R^2 = 0.69$) a L-glutamate transporter with a maximal rate of uptake of 25.1 pmol L-Glu mg protein^{-1} min^{-1} and a substrate concentration giving 50% of maximal uptake rate of 2.87 μM (Figure 7). The overlap of the two kinetic curves of the putative transporters complicates interpretations of their properties, so only the more strongly supported transporter acting at concentrations below 10 μM L-glutamate will be discussed. The kinetic parameters previously stated were determined using a sigmoidal model based on the Hill equation, which generally reflects transport processes that involve the binding of a co-transported substance (Lolkema and Slotboom 2015). A Lineweaver-Burk plot was also created for the data to compare parameter estimates assuming the underlying transport obeys Michaelis-Menten kinetics with just a single substrate binding to the transporter (Lineweaver and Burk 1934). This analysis gave a K_m of 13.54 μM and a J_{max} of 25.64 pmol L-glutamate mg^{-1}

min^{-1} (Figure S3). While the two J_{max} estimates of these approaches are very similar, the K_m estimates differ dramatically. The Lineweaver-Burk plot has a negative y-intercept for the linear regression, which does not normally occur with enzymes or transporters that follow Michaelis-Menton kinetics. This therefore suggests that the L-glutamate transport mechanism is dependent on the binding of another ligand, most likely either a positively charged ion brought in via symport with L-glutamate or a negatively charged ion exiting the cell via antiport.

The K_m of the putative transporter functional at lower L-Glu concentrations shows a high affinity for its substrate compared to other examined invertebrate epithelial amino acid transport systems (Figure 14). The sea urchin *Paracentrotus livitus* takes up L-valine with a K_m of 13.8 µM, while the spat larvae of the oyster *Ostrea edulis* takes up L-alanine with a K_m of 16.8 µM (Rice et al. 1980, Allemand et al. 1988). However, the estuarine green shore crab *Carcinus meanas* takes up L-leucine with a K_m of 1.7 µM (Blewett and Goss 2017), suggesting that the observed substrate affinity of the *E. muelleri* uptake is not outside of the previously documented range of amino acid transporter affinity. The *E. muelleri* transporter K_m also is comparable to the K_m determined for human excitatory amino acid transporters (EAAT), with a K_m for L-glutamate of 9 µM and 2.5 µM for EAAT3 and EAAT4, respectively (Lin et al. 2001, Mim et al. 2005). However, the *E. muelleri* transporter shows an almost 10-fold greater affinity for L-glutamate than previously documented L-glutamate transporters in other invertebrates, with the K_m of L-glutamate transport in the parasitic platyhelminth *Echinococcus granulosus* of 28 µM and a K_m of 29.4 µM for L-glutamate uptake in the mosquito *Aedes aegypti* (Jeffs and Arme 1987, Umesh et al. 2003). The differences in affinity may reflect differences in the environment to which the transporters are exposed. The *E. muelleri* transporter would be exposed to the water circulating through the sponge, which is taken directly from the surrounding environment, while *E.*

granulosis would be exposed to the nutrient rich environment within its host and the *A. aegypti* transporter concentrated within the nervous system will be adjacent to immediate L-glutamate release (Jeffs and Arme 1987, Umesh et al. 2003). The lower K_m of the *E. muelleri* transporter thus may reflect an adaptation to the low L-glutamate concentrations commonly found within freshwater environments, which are on the scale of 1 μM (Abe and Wasa 1989, Hornak et al. 2016).

Comparisons of the J_{max} of the *E. muelleri* transporter with other organisms is complicated by a variance in the methodologies used when reporting and measuring uptake rates. This work used protein content of tissue as the means of standardization, but in other invertebrate studies other standards have been used including uptake per whole organism (Manahan et al. 1989, Epel 1972), per wet weight of the organism (Dean et al. 1987, Barber et al. 1989) , per cell (Umesh et al. 2003) or per volume of water passed through the system in perfusion setups (Blewett and Goss 2017). Initial comparison of the 25.1 pmol L-Glu mg protein^{-1} minute^{-1} L-Glu uptake rate of *E. muelleri* with the reported uptake rates of human EAAT3 and EAAT4 (1.02 nmol L-Glu mg protein^{-1} min^{-1} and 0.13 nmol L-Glu mg protein^{-1} min^{-1}, respectively) suggest that L-Glu uptake into *E. muelleri* has a maximal rate that is within an order of magnitude the reported physiological ranges in humans (Lin et al. 2001, Mim et al. 2005). In particular, the J_{max} of the *E. muelleri* transporter appears to only be 5-fold lower than the J_{max} for human EAAT4. However, a caveat to this analysis is that the uptake rate for the human EAAT4 was determined using heterologous expression in HEK 293 cells, so the overall expression of the protein relative to other proteins would not be the same as in the tissues where the transporter is normally expressed. Experiments using heterologous expression of the *E. muelleri* transporter in a system

such as *Xenopus* oocytes would form the basis for a more equitable comparison of the characteristics of the transport systems.

4.2 Inhibition and Ion Dependence:

L-glutamate uptake by *E. muelleri* was reduced by the presence of both L-aspartate and D-glutamate and may be reduced in the presence of L-alanine (Figure 8, S1). L-glutamate transporters in other organisms often also take up L-aspartate due to the similar charge and shape of L-aspartate relative to L-glutamate (Matsuo et al. 2002, Canul-Tec et al. 2017). L-alanine affecting L-glutamate uptake supports the possibility that L-glutamate uptake in *E. muelleri* may be part of broad specificity amino acid uptake. Further experiments examining the effect of other neutral amino acids on L-glutamate uptake are needed to confirm this. L-glutamate uptake being affected by L-aspartate suggests that the transporter acting within *E. muelleri* is most likely homologous to the SLC1 or SLC7 families, or to SLC17A5 (Table 2).

L-glutamate uptake in *E. muelleri* was not affected by depletion of calcium individually, but some effect on uptake was seen with depletion of sodium and simultaneous depletion of both ions (Figure 9, S2). Differences in the overall conclusion reached from separate experiments in sodium free media make it difficult to formulate an overall statement on the role of sodium in the transport mechanism. However, these results do support that L-glutamate uptake in *E. muelleri* is largely calcium independent. This in turn suggests that the L-Glu transporter in *E. muelleri* may have homology to SLC1 transporters, as SLC1 transporters are sodium dependent (Zerangue and Kavanaugh 1996). Vesicular glutamate transporters (SLC17, VGLUTs) are not dependent on sodium, so the *E. muelleri* transporter may also be homologous to this transporter family (Reimer and Edwards 2004). If L-glutamate uptake is truly independent from sodium concentrations this

may also reflect the lack of ions in freshwater environments. The sodium concentration in freshwater is on the order of 150 μM, while the concentration in saltwater is approximately 450 mM (Dugan et al. 2017, Emmanuel et al. 2012). Solutions used to test the kinetic parameters of mammalian SLC1 transporters used sodium concentrations of 140 mM (Grewer et al. 2000, Mim et al. 2005), which much more closely resembles the sodium content of saltwater than freshwater.

Calcium dependence of L-glutamate uptake has not been previously documented in other organisms, but the relative concentration of calcium in freshwater environments (on the order of 30 μM to 1.4 mM, Edwards et al. 2015) compared to previously measured intracellular calcium concentrations of near 150 nM (Garcia-Hirschfeld et al. 1995, Perovic et al. 1999) in several organisms opened the possibility that calcium cotransport may have been used in *E. muelleri* to drive uptake of L-glutamate into the sponge. There was no support for calcium dependence in these experiments, but there was some effect with removal of both sodium and calcium simultaneously. This may reflect dependence of L-glutamate uptake on one of sodium or calcium with the other ion being able to substitute as a transport substrate in cases of depletion. However, the continued uptake of L-glutamate even with depletion of both ions at almost 70% capacity suggests either the action of multiple transporters with only one transporter being ion dependent or the observed trend instead reflects natural variance in uptake rates.

L-glutamate uptake into *E. muelleri* was also not proton dependent, with both changes in media pH and application of the proton ionophore bafilomycin not affecting L-glutamate uptake rate (Figure 10). Proton dependence of uptake was investigated due to the utilization of protons to drive glutamate uptake by some previously documented transporters, including SLC17A5 (sialin) (Miyaji et al. 2008, Reimer 2013). Protons also represent a chemical gradient between

the freshwater environment and cells that could be used to drive L-glutamate uptake in the absence of high concentrations of other ions. These experiments did not support proton dependence of L-glutamate uptake, suggesting that a homolog of sialin is likely not responsible for L-glutamate uptake by *E. muelleri*.

Several other ions may also contribute to L-glutamate transport in *E. muelleri*. Potassium ions are exported during L-glutamate transport by SLC1 transporters (Kanai et al. 2013), so an experiment utilizing a potassium ionophore such as valinomycin or nigericin could be performed to break down any potassium ion gradient between sponge cells and the surrounding medium (Daniele and Holian 1976, Daniele et al. 1978). Chloride ion export is used in the transport mechanism of VGLUTs (Reimer 2013), and chloride ionophores related to valinomycin could be used to investigate the importance of chloride in L-glutamate transport in *E. muelleri* (Wu et al. 2016). Magnesium ions are another possible source of an ionic gradient to drive transport in freshwater environments. However, no known L-glutamate transporters in animals are dependent on divalent cations as a co-transported ion (Kanai et al. 2013, Fotiadis et al. 2013, Reimer 2013). Magnesium substitution could be performed similarly to how calcium substitution was previously performed or utilizing a magnesium ionophore such as ETH 5214 (Blatter 1990).

4.3 *E. muelleri* L-glutamate transporter complement:

Analysis of the *E. muelleri* genome utilizing BLAST protocols identified two putative homologs of SLC1 transporters and 8 putative homologs of SLC17 transporters (Figure 11,12,13). In vertebrates SLC1 transporters are expressed by glial cells near synapses to deplete L-glutamate used for triggering action potentials (Kanai et al. 2013). SLC1 transporters are dependent on both protons and sodium for L-glutamate uptake and can take up L-aspartate

(Zerangue and Kavanaugh 1996, Canul-Tec et al. 2017). Alignment of the two identified *E. muelleri* SLC1A3 homologs with mammalian sequences found that the *E. muelleri* sequences were less than half the length of the mammalian sequences (Figure 12). This suggests that the *E. muelleri* sequences may not function in L-glutamate transport. Domain analysis of the proteins further supports this conclusion, as the *E. muelleri* sequences lack transmembrane regions found within the mammalian sequences and only have a portion of the sodium dicarboxylate symporter domain that is contained within the mammalian sequences (Figure S5). Previous analysis of the SLC complement across a variety of organisms found that placozoans also do not have SLC1 homologs, suggesting that SLC1 transporters may have originated with the development of nervous systems (Hoglund et al. 2011).

SLC17A5(sialin) is a vesicular transporter known for transport of sugar acids in a proton dependent manner. However, further analysis of SLC17A5 has found that it may also be acting as an L-glutamate and L-aspartate transporter (Miyaji et al. 2008). SLC17A6-8 (VGLUT) are associated with glutaminergic neurons but take up L-glutamate into vesicles rather than sequestering it from the extracellular space (Reimer 2013). In contrast to SLC1 transporters, SLC17 transporters are not sodium dependent or proton dependent but are instead chloride dependent (Reimer and Edwards 2004). Six of the eight putative *E. muelleri* SLC17 sequences are identified as SLC17A5 homologs using reciprocal BLAST, but within the overall SLC phylogeny all eight of the SLC17 *E. muelleri* sequences group with each other (Figure 11). It is difficult to determine why this may be occurring in this analysis since the phylogeny generated does not have branch lengths.

Alignment of the *E. muelleri* sequences with mammalian SLC17A5 and SLC17A7 sequences shows that the six *E. muelleri* sequences homologous to SLC17A5 are all near full

length relative to the mammalian sequences, while the VGLUT homologs are much smaller (Figure 13). This mirrors the trend seen in the SLC1 *E. muelleri* homologs, suggesting that these sequences may not be functional in L-glutamate transport. Domain analysis of the SLC17 homologs further confirmed this result, with the VGLUT homologs having only half the transmembrane regions compared to the other sequences and lacking the major facilitator superfamily domain at least partially present in all other sequences (Figure S6). This overall suggests that the only L-glutamate transporter within the *E. muelleri* genome is SLC17A5. The presence of six total copies of the gene is similar to trends seen in other sponges, where sponge species had duplicate copies of SLC17 sequences (Francis et al. 2017). Analyses of copy number of SLC17 genes in other animals have found that during vertebrate evolution additional copies of SLC17A5 genes were either lost or served as the basis for new SLC17 genes (Sreedharan et al. 2010). The scaffold placement and relative positioning of the *E. muelleri* SLC17 homologs suggests that both tandem duplication and chromosomal rearrangement may have contributed to the large number of sequences in *E. muelleri*. This overall complements the expansion of glutamate receptors seen in other sponge species to allow for the basis of a glutamate based signaling system (Abrams and Sossin 2018).

Only L-glutamate can be taken up by VGLUTs, so L-aspartate would not be expected to affect uptake rate if VGLUTs are the main transporters responsible (Reimer and Edwards 2004). Comparison of the functional characteristics of these transporters with the ion dependence and competitive inhibition experiments suggests that both SLC1 and SLC17 families of transporters may be responsible for the observed L-glutamate uptake. L-aspartate application would not lower VGLUT uptake rate, but SLC1 transporters would be dependent on sodium and/or proton concentration. However, examination of the *E. muelleri* genome did not find strong evidence for

sodium dependent L-glutamate transporters, in contrast to the possible sodium dependence seen within experimental data (Figure S2). An additional complication in interpreting the experimental results if only SLC17 transporters are found within *E. muelleri* is that SLC17 transporters are only found in membrane bound vesicles in cells in vertebrates (Reimer 2013). If SLC17 transporters are responsible for the L-glutamate uptake seen in *E. muelleri*, then the expression of SLC17 transporters would need to be at the cell membrane. One important caveat to this analysis is that the majority of functional characterization of SLC transporters has been performed in vertebrate model systems (Bai et al. 2017). The early divergence of sponges from other animals opens the possibility that the functionality of the transporter may also have greatly differentiated from vertebrate transporters (Mah and Leys 2017). The apparent absence of other L-glutamate transporters within the *E. muelleri* genome further supports this possibility. In-situ expression analysis of SLC17 transporter homologs will be needed to determine the extent to which this is occurring.

4.4 Contextualization of L-glutamate signaling

The *E. muelleri* sneeze response can be triggered by irritant application, mechanical stimulus, or application of concentrations of L-glutamate exceeding 70 μM (Elliott and Leys 2007, 2010). The experiments detailed above suggest that the high concentrations of L-glutamate required to trigger the sneeze response may be entering the sponge through diffusion rather than specific uptake (Figure 7). However, due to the limited number of L-glutamate concentrations tested it is also possible that a high capacity low affinity transporter may also be acting in this concentration range. Despite this, specific uptake of L-glutamate at low concentrations by *E. muelleri* is still occurring. One possibility for this specific uptake is for nutrient acquisition as

has been previously noted in other aquatic invertebrates (Wright and Manahan 1989). However, the demonstration by *E. muelleri* of an L-glutamate dependent behavior and the presence of VGLUT-like sequences in the *E. muelleri* genome suggests that observed L-glutamate uptake may instead be part of a coordination system in *E. muelleri*. The K_m is also similar to the EC_{50} of mammalian metabotropic glutamate receptors (mGluRs), which range between 100 nM and 1 mM (Reiner and Levitz 2018). The low environmental levels of L-glutamate would not allow for a direct trigger of the sneeze response by this uptake, but instead this uptake may be used to pool L-glutamate stores for release to trigger the response upon irritant application (Abe and Wasa 1989, Robarts et al. 1990, Hornak et al. 2016).

A coordination system based on L-glutamate in *E. muelleri* needs several different elements: receptors to bind L-glutamate, a way to terminate the signal upon completion of the response, and a source of signaling molecule. There are two main subsets of L-glutamate receptors, ionotropic receptors (iGluRs) and metabotropic receptors (mGluRs) (Barnard 1997, Conn and Pin 1997). Examination of sponge genomes has found some sponge species that have iGluRs (Class Homoscleromorpha and Calcarea), but all examined sponges have mGluRs (Riesgo et al. 2014, Francis et al. 2017, Ramos-Vicente et al. 2018). Copy number of mGluRs in sponges overall is lower than the 8 mGluRs found in vertebrates (Reiner and Levitz 2018). In *E. muelleri* this is in sharp contrast to the large number of VGLUT-like sequences available for L-glutamate transport (Figure 11). This suggests that a L-glutamate based signaling system would utilize control of available L-glutamate concentrations more heavily than differences in downstream receptor interacting proteins. Conversion of L-glutamate into GABA using glutamate decarboxylase may allow the use of GABA as a signal termination molecule within

the system, as a variety of examined sponge species express glutamate decarboxylase (Riesgo et al. 2014).

The coordination mechanism for the sneeze response in *E. muelleri* could thus work as follows: L-glutamate uptake would most likely occur along the choanocyte chambers of the sponge due to the large volumes of water passing through these chambers during normal filtration, but some uptake may also potentially occur over the exopinacoderm due to its direct contact with the water surrounding the sponge (Figure 15). The intake of L-glutamate could then be concentrated in the mesohyl, where motile cells expressing vesicular transporters could then sequester the L-glutamate into vesicles. One possible candidate cell type for this function is cystencytes, a motile cell in the mesohyl that has previously been demonstrated to contain large vesicles (Simpson 1984). Mechanical stimulation or presence of an irritant in the aquiferous system may then trigger release of L-glutamate vesicle contents into the mesohyl. The L-glutamate could then either directly diffuse to the osculum or enter the flow through the choanocyte chambers to reach the osculum. The osculum acts as the coordination center for the sneeze response, and removal of the osculum prevents functional propagation of the sneeze response (Ludeman et al. 2014). Previous work has also identified metabotropic glutamate receptors(mGluRs) in *E. muelleri* and other sponges, which trigger cAMP dependent signaling cascades in cells (Conn and Pin 1997, Riesgo et al. 2014, Leys et al. 2019b). Once mGluRs in the osculum have been activated, the sneeze response is then triggered and propagated through the body of the sponge. Application of high concentrations of L-glutamate in the sponge medium may bypass this normal mechanism by allowing diffusion to occur directly to the osculum. How the signal is propagated from the osculum to the rest of the sponge is currently unknown, but calcium waves likely play a role as the contraction wave seen during the sneeze response is

calcium dependent (Elliott and Leys 2010). These elements combined thus have the potential to allow for the whole-body coordination of *E. muelleri* and may also serve as a model for a possible way in which animal ancestors may have coordinated their body responses to changes in environmental conditions.

4.5 Conclusion:

The combined results of these experiments document uptake of L-glutamate by *E. muelleri* that shows a mixture of characteristics from several families of L-glutamate transporters. This uptake system may potentially serve as the basis for the coordination system involved in the sneeze response in *E. muelleri*. The capacity for amino acid uptake in a freshwater environment without a clear driving gradient is also of great physiological interest. Further experiments examining other potential driving ions such as chloride are needed to further characterize this system, and comparative analysis of the amino acid uptake capacity of other freshwater organisms across their extra-intestinal epithelia could provide insights into adaptations of animals to freshwater environments.

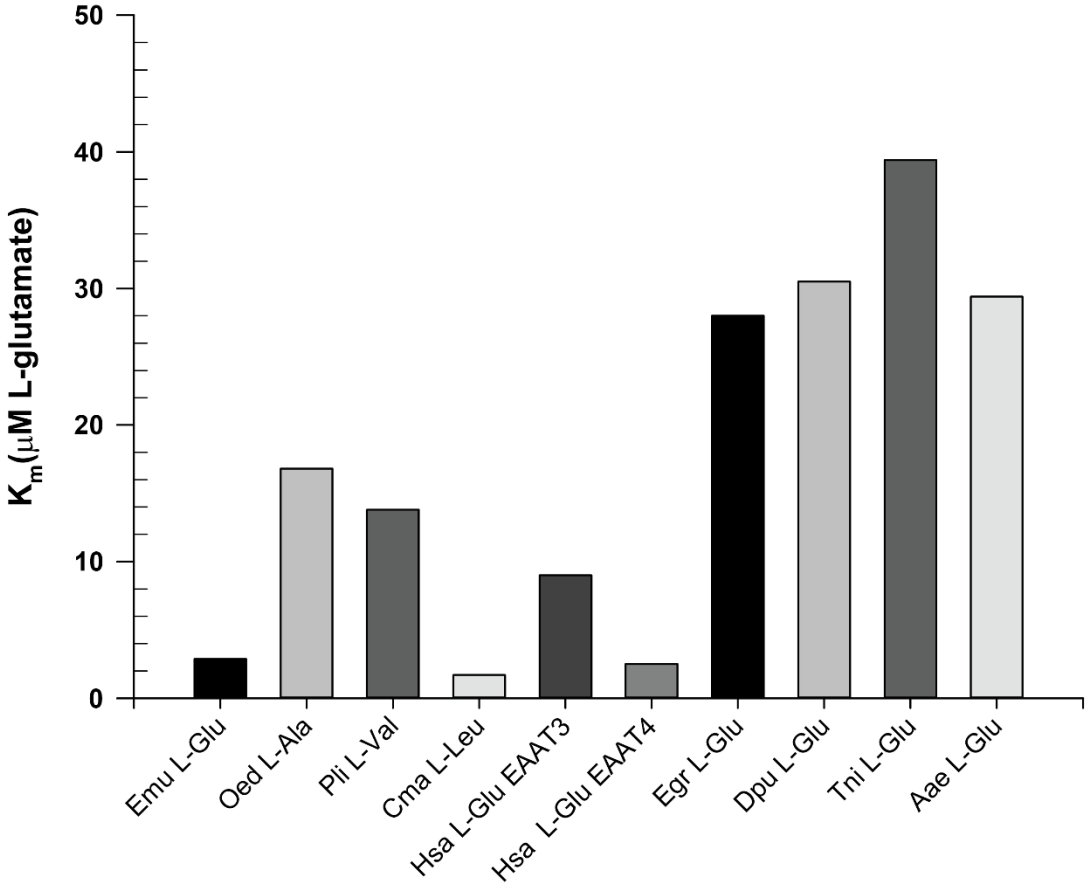
50
40
30
20
10
0
K_m(μM L-glutamate)
Emu L-Glu
Oed L-Ala
Pli L-Val
Cma L-Leu
Hsa L-Glu EAAT3
Hsa L-Glu EAAT4
Egr L-Glu
Dpu L-Glu
Tni L-Glu
Aae L-Glu

Figure 14: Comparison of the substrate concentration causing half the rate of maximal uptake (K_m) of amino acid transporters in a variety of organisms. Bars show mean reported value. Emu = *Ephydatia muelleri*, data sourced from above. Oed = *Ostrea edulis* larvae, sourced from Rice et al. 1980. Pli = *Paracentrotus livitus* larvae, sourced from Allemand et al. 1988. Cma = *Carcinus maenas* gills, sourced from Blewett and Goss 2017. Hsa = *Homo sapiens* neurons, EAAT3 data sourced from Lin et al. 2001 and EAAT4 data sourced from Mim et al. 2005. Egr = *Echinococcus granulosis*, data sourced from Jeffs and Arme 1987. Dpu = *Diploptera punctate*, Tni =*Trichoplusia ni*, Aae = *Aedes aegypti*, all sourced from Umesh et al. 2003.

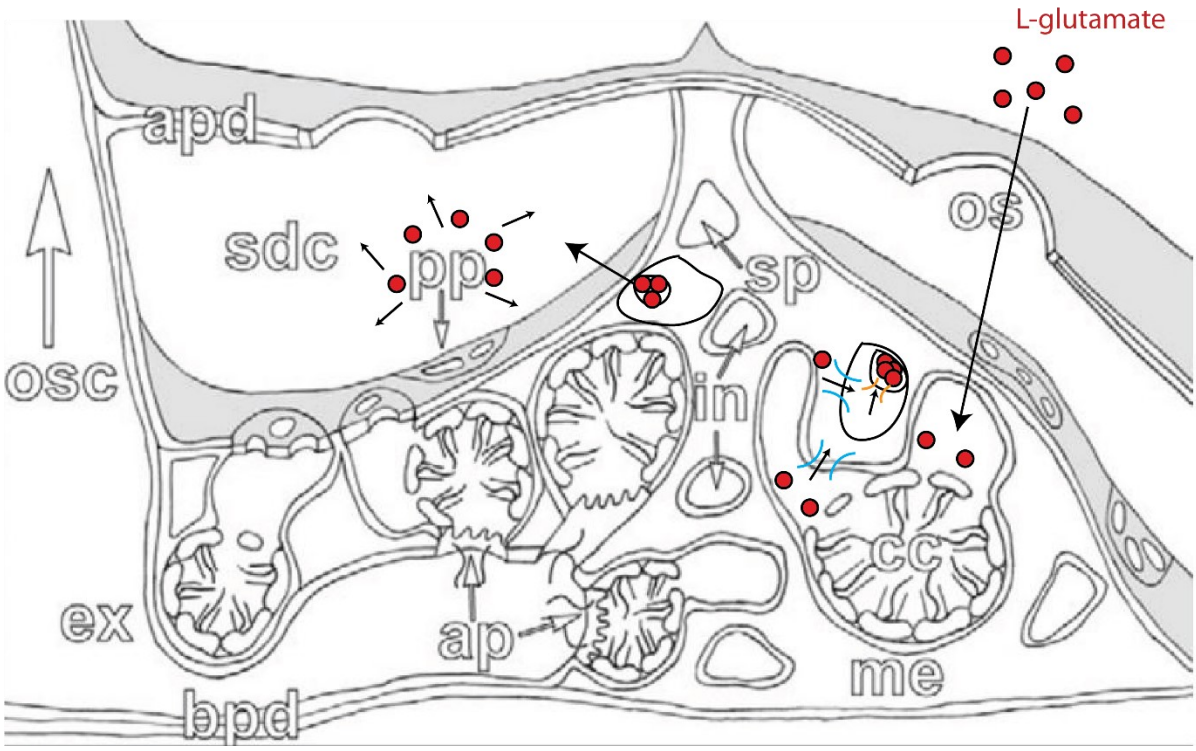
L-glutamate
apd
sdc
pp
sp
os
osc
in
cc
ex
ap
me
bpd

Figure 15: Proposed mechanism of coordination of the sneeze response of *E. muelleri* adapted from Elliott and Leys 2007. L-glutamate enters through the ostia into the choanocyte chambers, where it is transported into the mesohyl by one subset of L-glutamate transporters. Cells within the mesohyl expressing cell membrane transporters then sequester the L-glutamate and further concentrate it within vesicles using a different subset of L-glutamate transporters. Vibrations or clogging of the canal system triggers vesicle release, thus allowing the L-glutamate to diffuse throughout the mesohyl and bind to mGluRs.

Property	SLC1	SLC7A13	SLC17A5	SLC17A6-8	Putative *E. muelleri transporter*
Substrates transported	L-glutamate, D/L-aspartate (Kanai et al. 2013)	L-aspartate, L-glutamate (Fotiadis et al. 2013)	Acidic sugars, L-glutamate, L-aspartate (Miyaji et al. 2008, Reimer 2013)	L-glutamate (Reimer 2013)	L-glutamate, D-glutamate, L-aspartate, possibly L-alanine
Ions transported	Import: H^+, Na^+ Export: K^+ (Kanai et al. 2013)	None detected (Matsuo et al. 2002)	Import: H^+ (Reimer 2013)	Export: Cl^- (Reimer 2013)	Possibly Na^+ and Ca^{2+}
Cellular localization	Cell membrane (Kanai et al. 2013)	Cell membrane (Matsuo et al. 2002)	Lysosome and synaptic vesicles (Miyaji et al. 2008, Reimer 2013)	Synaptic vesicle (Reimer 2013)	unknown
K_m	0.6-10 µM (Grewer et al. 2000, Lin et al. 2001, Mim et al. 2005)	21.8 µM (Matsuo et al. 2002)	Approximately 500 µM (Miyaji et al. 2008)	1.2-2 mM (Bellocchio et al. 2000, Bai et al. 2001)	2.87 µM

Table 2: Comparison of properties of known L-glutamate transporters to experimental results of *E. muelleri* L-glutamate uptake. Sources of information for each individual cell are referenced within that cell.

Works Cited:

Abe, I., and T. Wasa. 1989. Gas-chromatographic determination of amino-acids in river water by enantiomer labeling. *Hrc-Journal of High Resolution Chromatography* 12 (10):661-664.

Abrams, Thomas W., and Wayne Sossin. 2018. Invertebrate Genomics Provide Insights into the Origin of Synaptic Transmission. In, ed Oxford University Press.

Adams, E. D. M., G. G. Goss, and S. P. Leys. 2010. Freshwater Sponges Have Functional, Sealing Epithelia with High Transepithelial Resistance and Negative Transepithelial Potential. *Plos One* 5 (11): 1-7.

Allemand, D., G. Derenzis, P. Payan, J. P. Girard, and R. Vaissiere. 1988. HgCl2-induced cell injury - differential-effects on membrane-located transport-systems in unfertilized and fertilized sea-urchin eggs. *Toxicology* 50 (2):217-230.

Altschul, S. F., W. Gish, W. Miller, E. W. Myers, and D. J. Lipman. 1990. Basic local alignment search tool. *Journal of Molecular Biology* 215 (3):403-410.

Anctil, M., I. Poulain, and C. Pelletier. 2005. Nitric oxide modulates peristaltic muscle activity associated with fluid circulation in the sea pansy *Renilla koellikeri*. *Journal of Experimental Biology* 208 (10):2005-2017.

Bai, L. Q., H. Xu, J. F. Collins, and F. K. Ghishan. 2001. Molecular and functional analysis of a novel neuronal vesicular glutamate transporter. *Journal of Biological Chemistry* 276 (39):36764-36769.

Bai, X. Y., T. F. Moraes, and R. A. F. Reithmeier. 2017. Structural biology of solute carrier (SLC) membrane transport proteins. *Molecular Membrane Biology* 34 (1-2):1-32.

Barber, A., J. I. Dean, R. Jordana, and F. Ponz. 1989. Sugar and amino-acid intestinal transport-systems in land snail *Helix-aspersa*. *Revista Espanola De Fisiologia* 45:215-224.

Barnard, E. A. 1997. Ionotropic glutamate receptors: New types and new concepts. *Trends in Pharmacological Sciences* 18 (5):141-148.

Bellocchio, E. E., R. J. Reimer, R. T. Fremeau, and R. H. Edwards. 2000. Uptake of glutamate into synaptic vesicles by an inorganic phosphate transporter. *Science* 289 (5481):957-960.

Blatter, L. A. 1990. Intracellular free magnesium in frog skeletal-muscle studied with a new type of magnesium-selective microelectrode - interactions between magnesium and sodium in the regulation of [Mg]i. *Pflugers Archiv-European Journal of Physiology* 416 (3):238-246.

Blewett, Tamzin A., and Greg G. Goss. 2017. A novel pathway of nutrient absorption in crustaceans: branchial amino acid uptake in the green shore crab (*Carcinus maenas*). *Proceedings of the Royal Society B-Biological Sciences* 284 (1868): 1-6.

Buck, M., and D. Schlichter. 1987. Driving forces for the uphill transport of amino-acids into epidermal brush-border membrane-vesicles of the sea-anemone, *Anemonia-sulcata* (Cnidaria, Anthozoa). *Comparative Biochemistry and Physiology a-Molecular & Integrative Physiology* 88 (2):273-279.

Canul-Tec, J. C., R. Assal, E. Cirri, P. Legrand, S. Brier, J. Chamot-Rooke, and N. Reyes. 2017. Structure and allosteric inhibition of excitatory amino acid transporter 1. *Nature* 544 (7651):446-451.

Capella-Gutierrez, Salvador, Jose M. Silla-Martinez, and Toni Gabaldon. 2009. trimAl: a tool for automated alignment trimming in large-scale phylogenetic analyses. *Bioinformatics* 25 (15):1972-1973.

Conn, P. J., and J. P. Pin. 1997. Pharmacology and functions of metabotropic glutamate receptors. *Annual Review of Pharmacology and Toxicology* 37:205-237.

Daniele, R. P., and S. K. Holian. 1976. Potassium ionophore (valinomycin) inhibits lymphocyte-proliferation by its effects on cell-membrane. *Proceedings of the National Academy of Sciences of the United States of America* 73 (10):3599-3602.

Daniele, R. P., S. K. Holian, and P. C. Nowell. 1978. Potassium ionophore (nigericin) inhibits stimulation of human lymphocytes by mitogens. *Journal of Experimental Medicine* 147 (2):571-581.

Dean, J. I., A. Barber, and F. Ponz. 1987. Neutral amino-acid-transport by snail (*Helix-aspersa*) intestine. *Comparative Biochemistry and Physiology a-Physiology* 87 (3):573-577.

Dellaporta, S. L., A. Xu, S. Sagasser, W. Jakob, M. A. Moreno, L. W. Buss, and B. Schierwater. 2006. Mitochondrial genome of *Trichoplax adhaerens* supports Placozoa as the basal lower metazoan phylum. *Proceedings of the National Academy of Sciences of the United States of America* 103 (23):8751-8756.

Dewaele, J. P., M. Anctil, and M. Carlberg. 1987. Biogenic catecholamines in the cnidarian *Renilla-kollikeri* - radioenzymatic and chromatographic detection. *Canadian Journal of Zoology-Revue Canadienne De Zoologie* 65 (10):2458-2465.

Dietz, T. H. 1979. Uptake of sodium and chloride by freshwater mussels. *Canadian Journal of Zoology-Revue Canadienne De Zoologie* 57 (1):156-160.

Dugan, H. A., S. L. Bartlett, S. M. Burke, J. P. Doubek, F. E. Krivak-Tetley, N. K. Skaff, J. C. Summers, K. J. Farrell, I. M. McCullough, A. M. Morales-Williams, D. C. Roberts, Z. Ouyang, F. Scordo, P. C. Hanson, and K. C. Weathers. 2017. Salting our freshwater lakes. *Proceedings of the National Academy of Sciences of the United States of America* 114 (17):4453-4458.

Dzubay, J. A., and C. E. Jahr. 1999. The concentration of synaptically released glutamate outside of the climbing fiber-Purkinje cell synaptic cleft. *Journal of Neuroscience* 19 (13):5265-5274.

Edwards, B. A., D. A. Jackson, and K. M. Somers. 2015. Evaluating the effect of lake calcium concentration on the acquisition of carapace calcium by freshwater crayfish. *Hydrobiologia* 744 (1):91-100.

El-Gebali, S., J. Mistry, A. Bateman, S. R. Eddy, A. Luciani, S. C. Potter, M. Qureshi, L. J. Richardson, G. A. Salazar, A. Smart, E. L. L. Sonnhammer, L. Hirsh, L. Paladin, D. Piovesan, S. C. E. Tosatto, and R. D. Finn. 2019. The Pfam protein families database in 2019. *Nucleic Acids Research* 47 (D1): D427-D432.

Elliott, G. R. D., and S. P. Leys. 2007. Coordinated contractions effectively expel water from the aquiferous system of a freshwater sponge. *Journal of Experimental Biology* 210 (21):3736-3748.

Elliott, G. R. D., and S. P. Leys. 2010. Evidence for glutamate, GABA and NO in coordinating behaviour in the sponge, *Ephydatia muelleri* (Demospongiae, Spongillidae). *Journal of Experimental Biology* 213 (13):2310-2321.

Ellwanger, K., A. Eich, and M. Nickel. 2007. GABA and glutamate specifically induce contractions in the sponge *Tethya wilhelma*. *Journal of Comparative Physiology a-Neuroethology Sensory Neural and Behavioral Physiology* 193 (1):1-11.

Ellwanger, Kornelia, and Michael Nickel. 2006. Neuroactive substances specifically modulate rhythmic body contractions in the nerveless metazoan *Tethya wilhelma* (Demospongiae, Porifera). *Frontiers in zoology* 3(7): 1-14.

Emmanuel, Akinsola Olufemi, Fatokun Ajibola Oladipo, and Ogunsanmi Olabode E. 2012. Investigation of salinity effect on compressive strength of reinforced concrete. *Journal of Sustainable Development* 5 (6):74-82.

Epel, D. 1972. Activation of an Na+-dependent amino-acid transport-system upon fertilization of sea-urchin eggs. *Experimental Cell Research* 72 (1):74-89.

Fotiadis, Dimitrios, Yoshikatsu Kanai, and Manuel Palacin. 2013. The SLC3 and SLC7 families of amino acid transporters. *Molecular Aspects of Medicine* 34 (2-3):139-158.

Francis, Warren R., Michael Eitel, Sergio Vargas, Marcin Adamski, Steven H.D. Haddock, Stefan Krebs, Helmut Blum, Dirk Erpenbeck, and Gert Worheide. 2017. The genome of the contractile demosponge *Tethya wilhelma* and the evolution of metazoan neural signalling pathways. *BioRxiv*. 1-25. doi: http://dx.doi.org/10.1101/120998.

Fredriksson, R., K. J. V. Nordstrom, O. Stephansson, M. G. A. Hagglund, and H. B. Schioth. 2008. The solute carrier (SLC) complement of the human genome: Phylogenetic classification reveals four major families. *Febs Letters* 582 (27):3811-3816.

Funayama, N., M. Nakatsukasa, T. Hayashi, and K. Agata. 2005. Isolation of the choanocyte in the freshwater sponge, *Ephydatia fluviatilis* and its lineage marker, Ef annexin. *Development Growth & Differentiation* 47 (4):243-253.

Gajewski, M., C. Schmutzler, and G. Plickert. 1998. Structure of neuropeptide precursors in cnidaria. *Trends in Comparative Endocrinology and Neurobiology: from Molecular to Integrative Biology* 839 (1):311-315.

Garcia-Hirschfeld, J., L. G. Lopez-Briones, C. Belmonte, and M. Valdeolmillos. 1995.
Intracellular free calcium responses to protons and capsaicin in cultured trigeminal neurons. *Neuroscience* 67 (1):235-243.

Glover, C. N., C. Bucking, and C. M. Wood. 2011. Adaptations to in situ feeding: novel nutrient acquisition pathways in an ancient vertebrate. *Proceedings of the Royal Society B-Biological Sciences* 278 (1721):3096-3101.

Goldstein, Josephine, Nickles Bisbo, Peter Funch, and Hans Ulrik Riisgard. 2020. Contraction-Expansion and the Effects on the Aquiferous System in the Demosponge Halichondria panicea. *Frontiers in Marine Science* 7.

Grant, N., E. Matveev, A. S. Kahn, S. K. Archer, A. Dunham, R. J. Bannister, D. Eerkes-Medrano, and S. P. Leys. 2019. Effect of suspended sediments on the pumping rates of three species of glass sponge in situ. *Marine Ecology Progress Series* 615:79-100.

Grewer, C., N. Watzke, M. Wiessner, and T. Rauen. 2000. Glutamate translocation of the neuronal glutamate transporter EAAC1 occurs within milliseconds. *Proceedings of the National Academy of Sciences of the United States of America* 97 (17):9706-9711.

Hertz, Leif. 2013. The Glutamate-Glutamine (GABA) Cycle: Importance of Late Postnatal Development and Potential Reciprocal Interactions between Biosynthesis and Degradation. *Frontiers in Endocrinology* 4:59.

Hoglund, P. J., K. J. V. Nordstrom, H. B. Schioth, and R. Fredriksson. 2011. The Solute Carrier Families Have a Remarkably Long Evolutionary History with the Majority of the Human Families Present before Divergence of Bilaterian Species. *Molecular Biology and Evolution* 28 (4):1531-1541.

Hornak, K., H. Schmidheiny, and J. Pernthaler. 2016. High-throughput determination of dissolved free amino acids in unconcentrated freshwater by ion-pairing liquid

chromatography and mass spectrometry. *Journal of Chromatography A* 1440:85-93.
Horne, F. R. 1967. Active uptake of sodium by freshwater notostracan *Triops longicaudatus*. *Comparative Biochemistry and Physiology* 21 (3):525-531.
Jager, M., R. Chiori, A. Alie, C. Dayraud, E. Queinnec, and M. Manuel. 2011. New Insights on Ctenophore Neural Anatomy: Immunofluorescence Study in *Pleurobrachia pileus* (Muller, 1776). *Journal of Experimental Zoology Part B-Molecular and Developmental Evolution* 316B (3):171-187.
Jeffs, S. A., and C. Arme. 1987. *Echinococcus-granulosus* - specificity of amino-acid transport-systems in protoscoleces. *Parasitology* 95 (1):71-78.
Jing, J., V. Alexeeva, S. A. Chen, K. Yu, M. R. Due, L. N. Tan, T. T. Chen, D. D. Liu, E. C. Cropper, F. S. Vilim, and K. R. Weiss. 2015. Functional Characterization of a Vesicular Glutamate Transporter in an Interneuron That Makes Excitatory and Inhibitory Synaptic Connections in a Molluscan Neural Circuit. *Journal of Neuroscience* 35 (24):9137-9149.
Jones, D. T., W. R. Taylor, and J. M. Thornton. 1992. The rapid generation of mutation data matrices from protein sequences. *Computer Applications in the Biosciences* 8 (3):275-282.
Kanai, Y., and M. A. Hediger. 2004. The glutamate/neutral amino acid transporter family SLC1: molecular, physiological and pharmacological aspects. *Pflugers Archiv-European Journal of Physiology* 447 (5):469-479.
Kanai, Y., B. Clemencon, A. Simonin, M. Leuenberger, M. Lochner, M. Weisstanner, and M. A. Hediger. 2013. The SLC1 high-affinity glutamate and neutral amino acid transporter family. *Molecular Aspects of Medicine* 34 (2-3):108-120.
Katoh, Kazutaka, John Rozewicki, and Kazunori D. Yamada. 2019. MAFFT online service: multiple sequence alignment, interactive sequence choice and visualization. *Briefings in Bioinformatics* 20 (4):1160-1166.
Kumar, Sudhir, Glen Stecher, and Koichiro Tamura. 2016. MEGA7: Molecular Evolutionary Genetics Analysis Version 7.0 for Bigger Datasets. *Molecular Biology and Evolution* 33 (7):1870-1874.
Kuznetsova, M., C. Lee, J. Aller, and N. Frew. 2004. Enrichment of amino acids in the sea surface microlayer at coastal and open ocean sites in the North Atlantic Ocean. *Limnology and Oceanography* 49 (5):1605-1619.
Leys, S. P., G. O. Mackie, and R. W. Meech. 1999. Impulse conduction in a sponge. *Journal of Experimental Biology* 202 (9):1139-1150.
Leys, Sally P., George O. Mackie, and Henry M. Reiswig. 2007. The biology of glass sponges. *Advances in Marine Biology, Vol 52* 52:1-145.
Leys, S. P., and A. Hill. 2012. The physiology and molecular biology of sponge tissues. *Advances in Sponge Science: Physiology, Chemical and Microbial Diversity, Biotechnology* 62:1-56.
Leys, S. P. 2015. Elements of a 'nervous system' in sponges. *Journal of Experimental Biology* 218 (4):581-591.
Leys, Sally, Lauren Grombacher, and April Hill (2019a). Hatching and freezing gemmules from the freshwater sponge *Ephydatia muelleri*. protocols.io dx.doi.org/10.17504/protocols.io.863hzgn
Leys, S. P., J. L. Mah, P. R. McGill, L. Hamonic, F. C. De Leo, and A. S. Kahn. 2019b. Sponge Behavior and the Chemical Basis of Responses: A Post-Genomic View. *Integrative and Comparative Biology* 59 (4):751-764.

Letunic, I., and P. Bork. 2018. 20 years of the SMART protein domain annotation resource. *Nucleic Acids Research* 46 (D1): D493-D496.

Lin, C. L. G., I. Orlov, A. M. Ruggiero, M. Dykes-Hoberg, A. Lee, M. Jackson, and J. D. Rothstein. 2001. Modulation of the neuronal glutamate transporter EAAC1 by the interacting protein GTRAP3-18. *Nature* 410 (6824):84-88.

Lineweaver, H., and D. Burk. 1934. The determination of enzyme dissociation constants. *Journal of the American Chemical Society* 56 (3):658-666.

Lolkema, J. S., and D. J. Slotboom. 2015. The Hill analysis and co-ion-driven transporter kinetics. *Journal of General Physiology* 145 (6):565-574.

Ludeman, D. A., N. Farrar, A. Riesgo, J. Paps, and S. P. Leys. 2014. Evolutionary origins of sensation in metazoans: functional evidence for a new sensory organ in sponges. *BMC Evolutionary Biology* 14 (3): 1-10.

Mackie, G. O., I. D. Lawn, and M. P. Dececcatty. 1983. Studies on hexactinellid sponges .2. excitability, conduction and coordination of responses in *Rhabdocalyptus-dawsoni* (lambe, 1873). *Philosophical Transactions of the Royal Society of London Series B-Biological Sciences* 301 (1107):401-418.

Madeira, F., Y. M. Park, J. Lee, N. Buso, T. Gur, N. Madhusoodanan, P. Basutkar, A. R. N. Tivey, S. C. Potter, R. D. Finn, and R. Lopez. 2019. The EMBL-EBI search and sequence analysis tools APIs in 2019. *Nucleic Acids Research* 47 (W1): W636-W641.

Mah, J. L., and S. P. Leys. 2017. Think like a sponge: The genetic signal of sensory cells in sponges. *Developmental Biology* 431 (1):93-100.

Manahan, D. T., W. B. Jaeckle, and S. D. Nourizadeh. 1989. Ontogenic changes in the rates of amino-acid transport from seawater by marine invertebrate larvae (Echinodermata, Echiura, Mollusca). *Biological Bulletin* 176 (2):161-168.

Matsuo, H., Y. Kanai, J. Y. Kim, A. Chairoungdua, D. K. Kim, J. Inatomi, Y. Shigeta, H. Ishimine, S. Chaekuntode, K. Tachampa, H. W. Choi, E. Babu, J. Fukuda, and H. Endou. 2002. Identification of a novel Na+-independent acidic amino acid transporter with structural similarity to the member of a heterodimeric amino acid transporter family associated with unknown heavy chains. *Journal of Biological Chemistry* 277 (23):21017-21026.

Mim, C., P. Balani, T. Rauen, and C. Grewer. 2005. The glutamate transporter subtypes EAAT4 and EAATs 1-3 transport glutamate with dramatically different kinetics and voltage dependence but share a common uptake mechanism. *Journal of General Physiology* 126 (6):571-589.

Miyaji, T., N. Echigo, M. Hiasa, S. Senoh, H. Omote, and Y. Moriyama. 2008. Identification of a vesicular aspartate transporter. *Proceedings of the National Academy of Sciences of the United States of America* 105 (33):11720-11724.

Moussawi, Khaled, Arthur Riegel, Satish Nair, and Peter W. Kalivas. 2011. Extracellular glutamate: functional compartments operate in different concentration ranges. *Frontiers in Systems Neuroscience* 5:94-94.

Morgan, I. J., W. T. W. Potts, and K. Oates. 1994. Intracellular ion concentrations in branchial epithelial-cells of brown trout (*Salmo trutta* L) determined by x-ray-microanalysis. *Journal of Experimental Biology* 194(1):139-151.

Moroz, L. L., K. M. Kocot, M. R. Citarella, S. Dosung, T. P. Norekian, I. S. Povolotskaya, A. P. Grigorenko, C. Dailey, E. Berezikov, K. M. Buckley, A. Ptitsyn, D. Reshetov, K. Mukherjee, T. P. Moroz, Y. Bobkova, F. H. Yu, V. V. Kapitonov, J. Jurka, Y. V. Bobkov, J. J. Swore, D. O. Girardo, A. Fodor, F. Gusev, R. Sanford, R. Bruders, E. Kittler, C. E. Mills, J. P. Rast, R. Derelle, V. V. Solovyev, F. A. Kondrashov, B. J. Swalla, J. V. Sweedler, E. I. Rogaev, K. M. Halanych, and A. B. Kohn. 2014. The ctenophore genome and the evolutionary origins of neural systems. *Nature* 510 (7503):109-114.

Moroz, L. L. 2015. Convergent evolution of neural systems in ctenophores. *Journal of Experimental Biology* 218 (4):598-611.

Murua, J. 2007. Differential sodium uptake kinetics in freshwater Atlantic salmon with alternative life histories. *Comparative Biochemistry and Physiology a-Molecular & Integrative Physiology* 146 (4): S84-S85.

Nickel, M. 2004. Kinetics and rhythm of body contractions in the sponge *Tethya wilhelma* (Porifera: Demospongiae). *Journal of Experimental Biology* 207 (26):4515-4524.

Nielsen, C. 2008. Six major steps in animal evolution: are we derived sponge larvae? *Evolution & Development* 10 (2):241-257.

Perovic, S., A. Krasko, I. Prokic, I. M. Muller, and W. E. G. Muller. 1999. Origin of neuronal-like receptors in Metazoa: cloning of a metabotropic glutamate GABA-like receptor from the marine sponge *Geodia cydonium*. *Cell and Tissue Research* 296 (2):395-404.

Qiu, Xue-Mei, Yu-Ying Sun, Xin-Yu Ye, and Zhong-Guang Li. 2020. Signaling Role of Glutamate in Plants. *Frontiers in Plant Science* 10.

Ramos-Vicente, D., J. Ji, E. Gratacos-Batlle, G. Gou, R. Reig-Viader, J. Luis, D. Burguera, E. Navas-Perez, J. Garcia-Fernandez, P. Fuentes-Prior, H. Escriva, N. Roher, D. Soto, and A. Bayes. 2018. Metazoan evolution of glutamate receptors reveals unreported phylogenetic groups and divergent lineage-specific events. *Elife* 7: 1-23.

Rasmont, R. 1961. A technique for rearing fresh-water sponges in a controlled environment English summ. *Ann Soc Roy Zool Belgique* 91 (2):147-155.

Reimer, R. J. 2013. SLC17: A functionally diverse family of organic anion transporters. *Molecular Aspects of Medicine* 34 (2-3):350-359.

Reimer, R. J., and R. H. Edwards. 2004. Organic anion transport is the primary function of the SLC17/type I phosphate transporter family. *Pflugers Archiv-European Journal of Physiology* 447 (5):629-635.

Reiner, A., and J. Levitz. 2018. Glutamatergic Signaling in the Central Nervous System: Ionotropic and Metabotropic Receptors in Concert. *Neuron* 98 (6):1080-1098.

Reiswig, H. M. 1975. Bacteria as food for temperate-water marine sponges. *Canadian Journal of Zoology-Revue Canadienne De Zoologie* 53 (5):582-589.

Reiswig, H. M., and T. L. Miller. 1998. Freshwater sponge gemmules survive months of anoxia. *Invertebrate Biology* 117 (1):1-8.

Rice, M. A., K. Wallis, and G. C. Stephens. 1980. Influx and net flux of amino-acids into larval and juvenile European flat oysters, *Ostrea-edulis* (L.). *Journal of Experimental Marine Biology and Ecology* 48 (1):51-59.

Riesgo, A., N. Farrar, P. J. Windsor, G. Giribet, and S. P. Leys. 2014. The Analysis of Eight Transcriptomes from All Poriferan Classes Reveals Surprising Genetic Complexity in Sponges. *Molecular Biology and Evolution* 31 (5):1102-1120.

Robarts, R. D., R. J. Wicks, and R. Gehr. 1990. Seasonal-changes in the dissolved free amino-acid and DOC concentrations in a hypertrophic African reservoir and its inflowing rivers. *Hydrobiologia* 199 (3):201-216.

Satterlie, R. A. 2015. Cnidarian Nerve Nets and Neuromuscular Efficiency. *Integrative and Comparative Biology* 55 (6):1050-1057.

Senatore, A., T. S. Reese, and C. L. Smith. 2017. Neuropeptidergic integration of behavior in *Trichoplax adhaerens*, an animal without synapses. *Journal of Experimental Biology* 220 (18):3381-3390.

Sica, D., and F. Zollo. 1977. Free amino acids in some sponges. *Biochemical Syst Ecol* 5 (2):129-131, illust.

Simion, P., H. Philippe, D. Baurain, M. Jager, D. J. Richter, A. Di Franco, B. Roure, N. Satoh, E. Queinnec, A. Ereskovsky, P. Lapebie, E. Corre, F. Delsuc, N. King, G. Worheide, and M. Manuel. 2017. A Large and Consistent Phylogenomic Dataset Supports Sponges as the Sister Group to All Other Animals. *Current Biology* 27 (7):958-967.

Simpson, T. L. 1984. The Cell Biology of Sponges. New York: Springer-Verlag.

Sreedharan, S., J. H. A. Shaik, P. K. Olszewski, A. S. Levine, H. B. Schioth, and R. Fredriksson. 2010. Glutamate, aspartate and nucleotide transporters in the SLC17 family form four main phylogenetic clusters: evolution and tissue expression. *BMC Genomics* 11 (17): 1-12.

Strekal, T. A., and McDiffett.Wf. 1974. Factors affecting germination, growth, and distribution of freshwater sponge, *Spongilla-fragilis* leidy (Porifera). *Biological Bulletin* 146 (2):267-278.

Taylor, P. M. 2014. Role of amino acid transporters in amino acid sensing. *American Journal of Clinical Nutrition* 99 (1):223S-230S.

Thomas, J. D. 1997. The role of dissolved organic matter, particularly free amino acids and humic substances, in freshwater ecosystems. *Freshwater Biology* 38 (1):1-36.

Umesh, A., B. N. Cohen, L. S. Ross, and S. S. Gill. 2003. Functional characterization of a glutamate/aspartate transporter from the mosquito *Aedes aegypti*. *Journal of Experimental Biology* 206 (13):2241-2255.

Ungemach, L. F., K. Souza, P. E. Fell, and S. H. Loomis. 1997. Possession and loss of cold tolerance by sponge gemmules: A comparative study. *Invertebrate Biology* 116 (1):1-5.

Vacelet, J., and N. Bouryesnault. 1995. Carnivorous sponges. *Nature* 373 (6512):333-335.

Whelan, N. V., K. M. Kocot, L. L. Moroz, and K. M. Halanych. 2015. Error, signal, and the placement of Ctenophora sister to all other animals. *Proceedings of the National Academy of Sciences of the United States of America* 112 (18):5773-5778.

Wright, S. H. 1988. Amino-acid transport in the gill epithelium of a marine bivalve. *Comparative Biochemistry and Physiology a-Physiology* 90 (4):635-641.

Wright, S. H., and D. T. Manahan. 1989. Integumental nutrient-uptake by aquatic organisms. *Annual Review of Physiology* 51:585-600.

Wu, Xin, Luke W. Judd, Ethan N. W. Howe, Anne M. Withecombe, Vanessa Soto-Cerrato, Hongyu Li, Nathalie Busschaert, Hennie Valkenier, Ricardo Perez-Tomas, David N. Sheppard, Yun-Bao Jiang, Anthony P. Davis, and Philip A. Gale. 2016. Nonprotonophoric Electrogenic Cl- Transport Mediated by Valinomycin-like Carriers. *Chem* 1 (1):127-146.

Zerangue, N., and M. P. Kavanaugh. 1996. Flux coupling in a neuronal glutamate transporter. *Nature* 383 (6601):634-637.

Supplementary Figures:

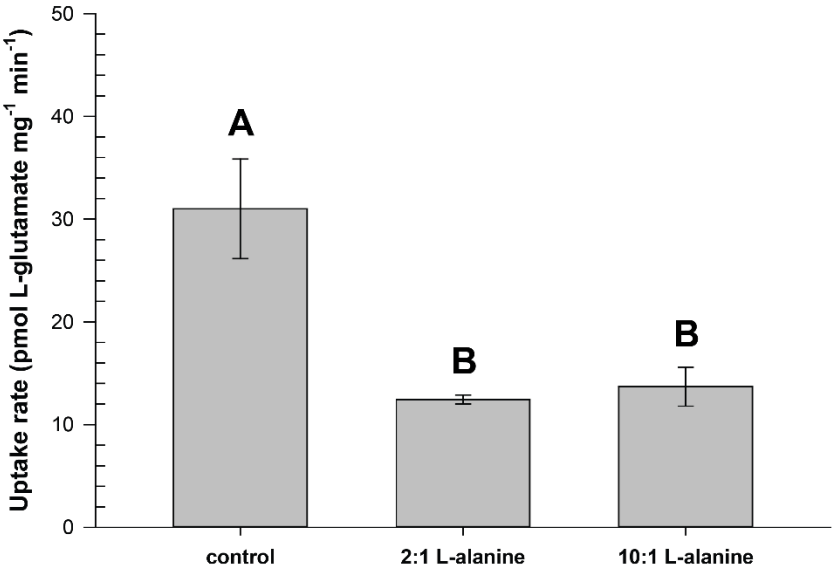

Figure S1: Additional experiment examining the effect of L-alanine on L-glutamate uptake by *E. muelleri*. Sponges were incubated in 6 µM L-glutamate for 16 hours. L-alanine was added at the same time as L-glutamate at either a 2:1 or 10:1 ratio. Values represent the mean ± standard error of the mean (S.E.M) of 5-6 replicates. Similar letters denote no significant difference between treatments, letters that are different indicate significant differences between treatments as determined by one-way ANOVA with Holm-Sidak post hoc tests at $\alpha = 0.05$.

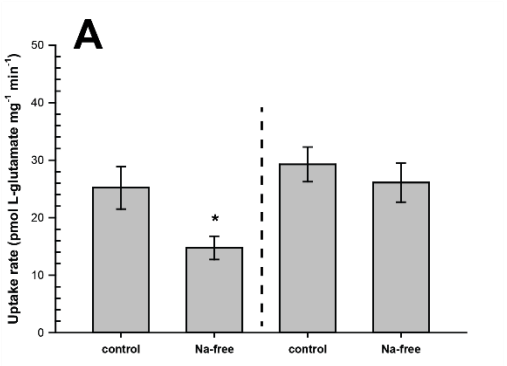
A
Uptake rate (pmol L-glutamate mg-1 min-1)
0
10
20
30
40
50
*
control
Na-free
control
Na-free

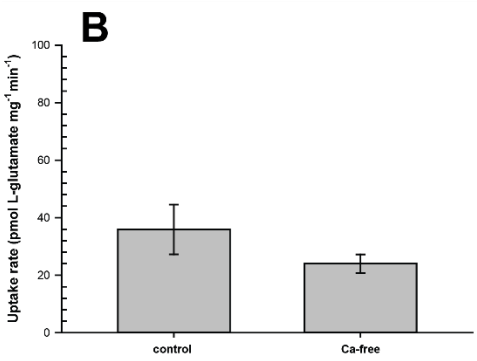
B
Uptake rate (pmol L-glutamate mg-1 min-1)
0
20
40
60
80
100
control
Ca-free

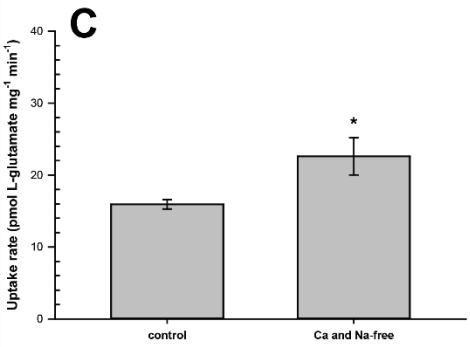
C
Uptake rate (pmol L-glutamate mg-1 min-1)
0
10
20
30
40
*
control
Ca and Na-free

Figure S2: Additional experiments examining the effect of ion substitution on L-glutamate uptake in *E. muelleri*. A: Uptake of L-glutamate in media with sodium substituted for N-methyl D-glucamine. The dashed line separates experiments run at different dates. B: Uptake of L-glutamate in media with calcium excluded without addition of EGTA. C: Uptake of L-glutamate in media reduced in both sodium and calcium. All incubation periods were 6 hours. Values indicate the mean ± standard error of the mean (S.E.M) of 7-9 replicates. Asterisks denote a significant difference between treatments as assessed by a two-tailed t-test at $\alpha = 0.05$.

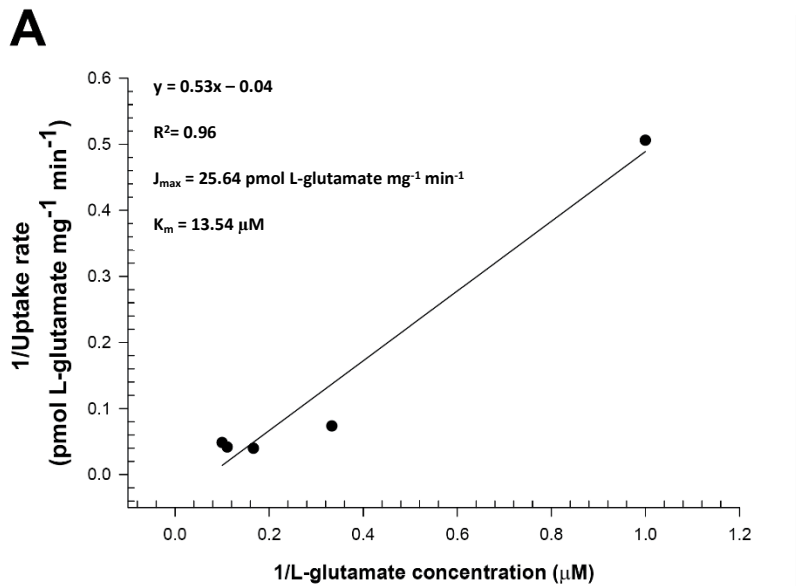
A
y = 0.53x – 0.04
R²= 0.96
Jmax = 25.64 pmol L-glutamate mg-1 min-1
Km = 13.54 µM
1/Uptake rate (pmol L-glutamate mg-1 min-1)
1/L-glutamate concentration (µM)
0.0
0.1
0.2
0.3
0.4
0.5
0.6
0.0
0.2
0.4
0.6
0.8
1.0
1.2

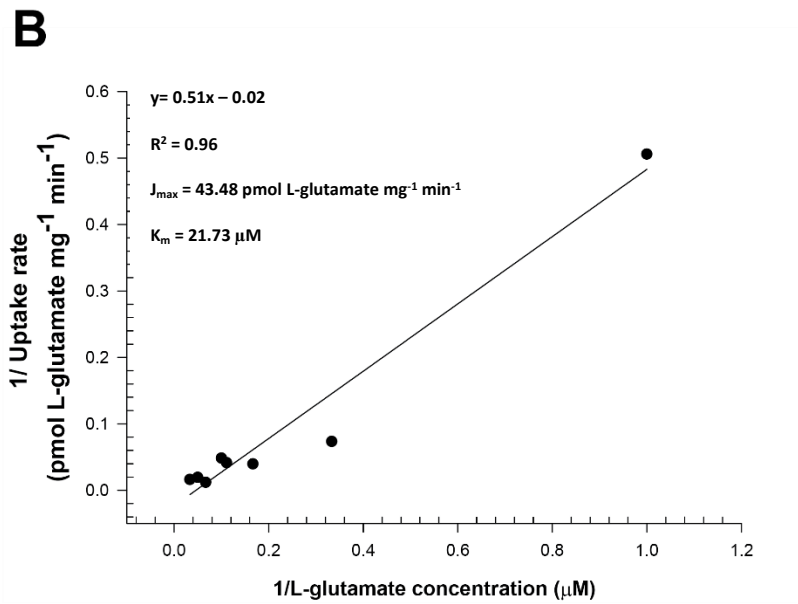
B
y= 0.51x – 0.02
R² = 0.96
Jmax = 43.48 pmol L-glutamate mg-1 min-1
Km = 21.73 µM
1/ Uptake rate (pmol L-glutamate mg-1 min-1)
1/L-glutamate concentration (µM)
0.0
0.1
0.2
0.3
0.4
0.5
0.6
0.0
0.2
0.4
0.6
0.8
1.0
1.2

Figure S3: Lineweaver-Burk plots of L-glutamate uptake below 10 μM L-glutamate (A) and below 30 μM L-glutamate (B). All incubation periods were for 16 hours. Values represent the inverse of the mean uptake rate of 4-9 replicates. Linear regression gives a line with the equation of $1/J = (K_m/J_{max})\ (1/S) + 1/J_{max}$. Reported J_{max} and K_m values are approximated from this equation.

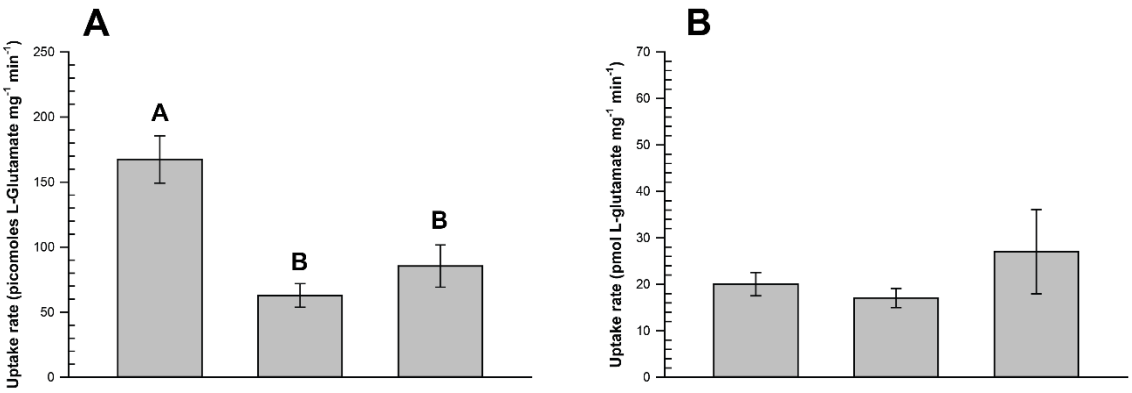
A
Uptake rate (picomoles L-Glutamate mg-1 min-1)
250
200
150
100
50
0
A
B
B
B
Uptake rate (pmol L-glutamate mg-1 min-1)
70
60
50
40
30
20
10
0

Figure S4: Variation in uptake rate of 30 µM (A) and 6 µM (B) L-glutamate by *E. muelleri* over a 16-hour incubation period between different experiments. Values represent the mean ± standard error of the mean (S.E.M) of 4-8 replicates. Similar letters denote no significant difference between treatments, letters that are different indicate significant differences between treatments as determined by one-way ANOVA with Holm-Sidak post hoc tests at $\alpha = 0.05$.

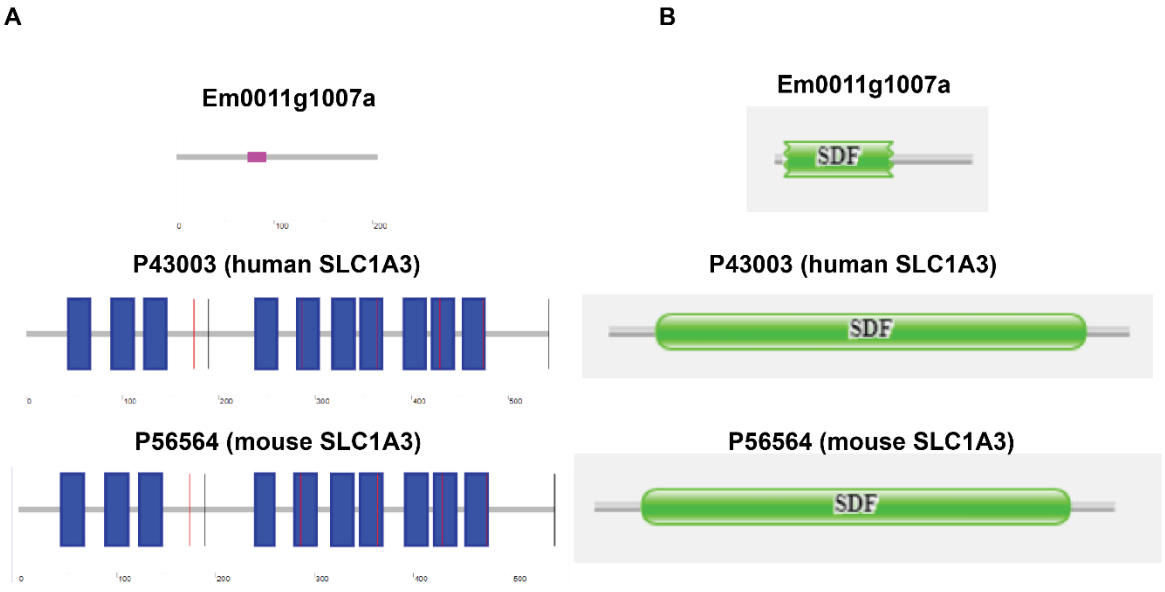
A
B
Em0011g1007a
Em0011g1007a
SDF
P43003 (human SLC1A3)
P43003 (human SLC1A3)
SDF
P56564 (mouse SLC1A3)
P56564 (mouse SLC1A3)
SDF

Figure S5: Domain composition of human and mouse SLC1 proteins compared to putative *E. muelleri* proteins. A: Domains identified by SMART (Letunic and Bork 2017). The small purple box is a region of low complexity, while blue boxes represent transmembrane regions. B: Domains identified by PFAM (El-Gabali et al. 2019). The SDF domain is for the sodium dicarboxylate symporter family.

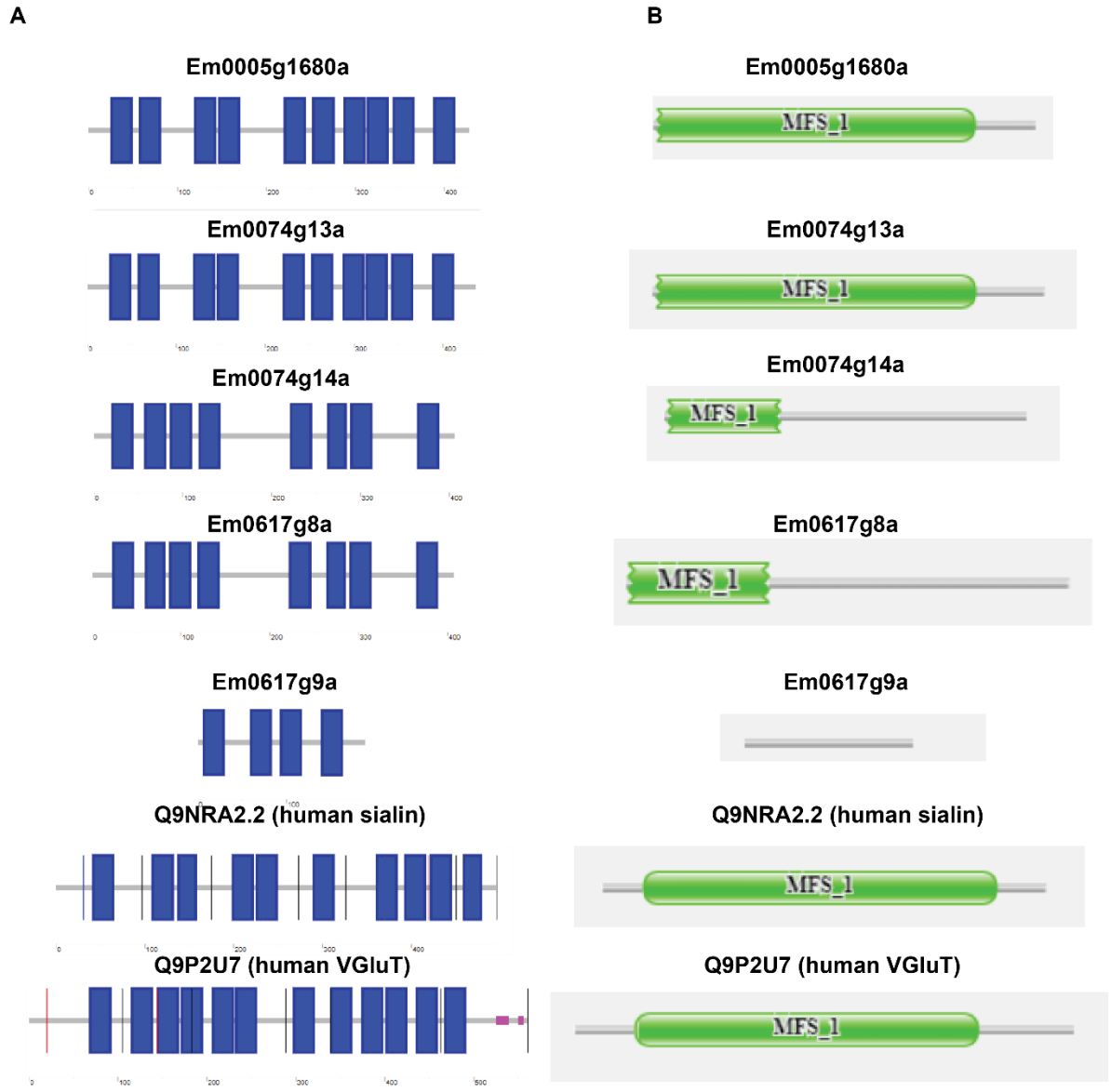
A
Em0005g1680a
Em0074g13a
Em0074g14a
Em0617g8a
Em0617g9a
Q9NRA2.2 (human sialin)
Q9P2U7 (human VGluT)
B
Em0005g1680a
MFS_1
Em0074g13a
MFS_1
Em0074g14a
MFS_1
Em0617g8a
MFS_1
Em0617g9a
Q9NRA2.2 (human sialin)
MFS_1
Q9P2U7 (human VGluT)
MFS_1

Figure S6: Domain composition of human and mouse SLC17 proteins compared to putative *E. muelleri* proteins. A: Domains identified by SMART (Letunic and Bork 2017). The small purple box is a region of low complexity, while blue boxes represent transmembrane regions. B: Domains identified by PFAM (El-Gabali et al. 2019). The MFS_1 domain is for the major facilitator superfamily.

Gene name	Query Sequence length (amino acids)	Hit ID	Query E value	Hit sequence length (amino acids)	Reverse blast hit	description	reverse E value
SLC1	543	Em0011g1007a	2E-15	205	NP_001276869.1	excitatory amino acid transporter 1 isoform 5 [Homo sapiens]	3.14E-22
SLC1	543	Em0011g994a	(2E-15)	205	NP_001276869.1	excitatory amino acid transporter 1 isoform 5 [Homo sapiens]	3.14E-22
First non-homolog	543	Em0413g2a	6.1	961	EAW82343.1	hCG2041486, partial [Homo sapiens]	0.001
SLC3	685	Em0019g638a	5.00E-126	617	EAX00279.1	solute carrier family 3 member 1, isoform CRA_b [Homo sapiens]	3.00E-127
SLC3	685	Em0019g639a	(1E-124)	590	EAX00279.1	solute carrier family 3 member 1, isoform CRA_b [Homo sapiens]	2.46E-128

First non-homolog	685	Em0013g851a	0.04	307	6R7I_A	Chain A, COP9 signalosome complex subunit 1 [Homo sapiens]	6e-129
SLC7	487	Em0018g1109a	6.00E-81	391	XP_016881719.1	B (0, +)-type amino acid transporter 1 isoform X2 [Homo sapiens] (SLC7A9)	1.54E-82
First non-homolog	487	Em0001g322a	3.1	9087	XP_011537704.1	deleted in malignant brain tumors 1 protein isoform X16 [Homo sapiens]	9e-139
SLC17A5	495	Em0005g1680a	4.00E-101	428	NP_036566.1	sialin [Homo sapiens] (SLC17A5)	5.85E-108
SLC17A5	495	Em0074g13a	5e-101	437	NP_036566.1	sialin [Homo sapiens] (SLC17A5)	9.30E-108
SLC17A5	495	Em0005g1679a	5e-89	406	NP_036566.1	sialin [Homo sapiens] (SLC17A5)	1.12E-89
SLC17A5	495	Em0074g14a	5e-89	406	NP_036566.1	sialin [Homo sapiens] (SLC17A5)	1.12E-89

SLC17A5	495	Em0617g8a	2e-88	407	NP_036566.1	sialin [Homo sapiens] (SLC17A5)	5.48E-89
SLC17A5	495	Em0438g9a	2e-88	407	NP_036566.1	sialin [Homo sapiens] (SLC17A5)	5.48E-89
First non-homolog	495	Em0018g1141a	2e-10	322	EAW75316.1	chromosome 20 open reading frame 59, isoform CRA_c [Homo sapiens]	8e-22
SLC17A6-8	560	Em0617g9a	6e-27	188	NP_065079.1	vesicular glutamate transporter 2 [Homo sapiens]	4.98E-27
SLC17A6-8	560	Em0438g10a	6e-27	188	NP_065079.1	vesicular glutamate transporter 2 [Homo sapiens]	4.98E-27
First non-homolog	560	Em0018g1089a	9e-10	370	NP_071365.4	solute carrier family 17 member 9 isoform 1 [Homo sapiens]	3e-30

Table S1: Hit table of putative SLC genes in *E. muelleri* that may function as L-glutamate transporters. Gene identifiers used for *E. muelleri* sequences are from the *E. muelleri* genome annotation. Human SLC sequences were used for initial BLAST searches, and reverse blast was performed against human sequences within the nr database in NCBI. Following each gene family of interest is listed the first non-homologous *E. muelleri* sequences listed in initial search results using human queries. Non-homology was determined based on reverse blast returning a result not within the SLC family of interest.

Figure	Gemmule source used
5	A (most data), E (16-hour time point in 5C)
6	B (1 μM, 3 μM, 9 μM, and 60 μM), C (10 μM and 20 μM), D (15 μM), E (0 μM and 30 μM), F (6 μM)
7	F
8	F (sodium free and double substituted), G (calcium free)
9	F
S1	E
S2	F
S3	Same as 6 above
S4	B (30 μM data and leftmost 6 μM bar), F (middle and rightmost 6 μM bar)

Table S2: Individual sponges contributing to each previous figure. Separate adult sponge individuals are labeled with different capital letters. Sponges labeled A-D were collected from the head tank of the Victoria Capital Regional District water system in 2017 and sponges labeled E-G were collected from O'Connor Lake in 2018.